The genome of *Auriculariopsis ampla* sheds light on fruiting body development and wood-decay of bark-inhabiting fungi

Éva Almási[1]*, Neha Sahu[1]*, Krisztina Krizsán[1], Balázs Bálint[1], Gábor M. Kovács[2,3], Brigitta Kiss[1], Judit Cseklye[4], Elodie Drula[5,6], Bernard Henrissat[5,6,7], István Nagy[4], Mansi Chovatia[8], Catherine Adam[8], Kurt LaButti[8], Anna Lipzen[8], Robert Riley[8], Igor V. Grigoriev[8], László G. Nagy[1&]

[1]Synthetic and Systems Biology Unit, Institute of Biochemistry, Biological Research Center, HAS, Szeged, 6726, Hungary

[2]Department of Plant Anatomy, Institute of Biology, Eötvös Loránd University, Budapest, 1117, Hungary

[3]Plant Protection Institute, Centre for Agricultural Research, Hungarian Academy of Sciences, Budapest, 1022, Hungary

[4]Seqomics Ltd. Mórahalom, Mórahalom 6782, Hungary

[5]Architecture et Fonction des Macromolécules Biologiques (AFMB), CNRS, Université Aix-Marseille, 163 Avenue de Luminy, 13288, Marseille, France

[6]INRA, USC 1408 AFMB, 13288, Marseille, France

[7]Department of Biological Sciences, King Abdulaziz University, Jeddah, 21589, Saudi Arabia

[8]US Department of Energy Joint Genome Institute, 2800 Mitchell Drive, Walnut Creek, CA 94598 CA

* These authors contributed equally to this work.

24 &Author for correspondence: László G. Nagy e-mail: lnagy@fungenomelab.com

25

26 Abstract

27 The Agaricomycetes are fruiting body forming fungi that produce some of the most efficient
28 enzyme systems to degrade woody plant materials. Despite decades-long interest in the
29 ecological and functional diversity of wood-decay types and in fruiting body development, the
30 evolution of the genetic repertoires of both traits are incompletely known. Here, we sequenced
31 and analyzed the genome of *Auriculariopsis ampla*, a close relative of the model species
32 *Schizophyllum commune.* Comparative analyses of wood-decay genes in these and other 29
33 Agaricomycetes species revealed that the gene family composition of *A. ampla* and *S. commune*
34 are transitional between that of white rot species and less efficient wood-degraders (brown rot,
35 ectomycorrhizal). Rich repertoires of suberinase and tannase genes were found in both species,
36 with tannases generally restricted to species that preferentially colonize bark-covered wood.
37 Analyses of fruiting body transcriptomes in both *A. ampla* and *S. commune* highlighted a high
38 rate of divergence of developmental gene expression. Several genes with conserved
39 developmental expression were found, nevertheless, including 9 new transcription factors as well
40 as small secreted proteins, some of which may serve as fruiting body-specific effector molecules.
41 Taken together, the genome sequence and developmental transcriptome of *Auriculariopsis ampla*
42 has highlighted novel aspects of wood-decay diversity and of fruiting body development in
43 mushroom-forming fungi.

44

Introduction

Mushroom-forming fungi (Agaricomycetes) are of great interest for comparative genomics due to their importance as wood-degraders in global carbon cycling and as complex multicellular organisms that produce agriculturally or medicinally relevant fruiting bodies. Recent advances in genome sequencing has brought new light on several aspects of lignocellulose decomposition and the genetic repertoire of fruiting body development in mushroom-forming fungi [1–5].

The Agaricomycetes display diverse strategies to utilize lignocellulosic substrates. While genomic analyses have helped to uncover the main patterns of duplication and loss of plant cell wall degrading enzyme (PCWDE) families, our understanding of the enzymatic repertoires of Agaricomycetes and how they use it to degrade various lignocellulosic components of plants is far from complete. Fungi have traditionally been classified either as white rot, in which all components of the plant cell wall are being degraded [6], or brown rot, in which mostly cellulosic components are degraded, but lignin is left unmodified or only slightly modified [7]. Several species have been recalcitrant to such classification, which prompted a reconsideration of the boundaries of the classic WR and BR dichotomy [8,9]. Such species are found across the fungal phylogeny, but seem to be particularly common among early-diverging Agaricales, including the Schizophyllaceae, Fistulinaceae and Physalacriaceae [2,8,9]. *Schizophyllum commune*, the only hitherto genome-sequenced species in the Schizophyllaceae, for example, produces white rot like symptoms, but lacks hallmark gene families (e.g. lignin-degrading peroxidases) of WR fungi [2,8–10]. Accordingly, it lacks the ability to degrade lignin and achieves weak degradation of wood [9,11,12], although this might be complemented by pathogenic potentials on living plants or the activity of other, more efficient degraders that co-inhabit the same substrate[13]. Analyses of the secretome and wood-decay progression of *S. commune* revealed both WR and BR-like behaviors [10,14], although several questions on the biology of this species remain open.

Fruiting body production, is a highly integrated developmental process triggered by a changing environment, such as a drop in temperature, nutrient depletion or shifts in light conditions [15–17]. It results from the concerted expression of structural and regulatory [1,18–22] genes as well as other processes, such as alternative splicing [3,23], allele-specific gene expression [3] and probably selective protein modification [3,24]. Known structural genes include hydrophobins [25–27] , lectins [28–30], several cell wall chitin and glucan-active CAZymes [5,31–33], and probably cerato-platanins, expansin-like [3,4] and an array of other genes [34]. Regulators of fruiting body development have been characterized in several species, in particular in *Coprinopsis cinerea* [18,19,35–37] and *S. commune* [1,2,24]. Despite much advance in this field, several aspects of fruiting body development are quite poorly known, including, for example what genes have conserved developmental roles across fruiting body forming fungi or how cell-cell communication is orchestrated in developing fruiting bodies. *S. commune* has served as a model organism for fruiting body development for a long time [2,15,16]. This species, like other Schizophyllaceae (e.g. the genus *Auriculariopsis*) produce cyphelloid fruiting bodies, which are reduced morphologies derived from more complex ancestors. Cyphelloid fruiting bodies are inverted cup-like forms with unstructured (e.g. *A. ampla*) or slightly structured (e.g. *S. commune*) spore-bearing surfaces (hymenophore). Albeit the hymenophore structure of *S. commune* resembles gills (hence the common name 'split gill'), it is not homologous to real gills of mushrooms, rather, it results from the congregation of several individual cup-like fruiting bodies.

We sequenced the genome of *Auriculariopsis ampla*, a close relative of *S. commune* that primarily inhabits the bark of dead logs and produces simple, cup-shaped fruiting bodies. Through analyses of gene repertoires for plant cell wall degradation in *A. ampla, S. commune* and 29 other Agaricomycetes, we detect signatures of adaptation to wood colonization through the bark and suggest that these two species have unusual plant cell wall degrading enzyme

93 repertoires. By sequencing developmental transcriptomes of *A. ampla* and comparing it to that of
94 *S. commune*, we identify conserved developmental genes that might be linked to fruiting body
95 development, including small secreted proteins, some of which show extreme expression
96 dynamics in fruiting bodies.

97

98 # Results and Discussion

99 ## *Auriculariopsis* has a typical Agaricales genome

100 The genome of *Auriculariopsis* was sequenced using PacBio, assembled to 49.8 Mb of DNA
101 sequence in 351 scaffolds with a mean coverage of 54.38x (343 scaffolds >2 kpb, N50: 19, L50:
102 0.53 Mb). We predicted 15,576 protein coding genes, based on which BUSCO analysis showed a
103 98.6% degree of completeness (273 complete, 28 duplicated, 2 fragmented, 2 missing). We
104 included *A. ampla* and its close relative *Schizophyllum commune* in a comparative analysis with
105 29 other Agaricomycetes. A species phylogeny was reconstructed from 362 single-copy
106 orthologs (14,2436 amino acid characters) for the 31 taxa; the inferred topology resembles
107 published genome-scale trees of Agaricomycetes very closely and received strong (>85%)
108 bootstrap support for all but two nodes (Figure 1a). *Auriculariopsis ampla* clustered with *S.*
109 *commune*, together representing the Schizophyllaceae, with their immediate neighbor being
110 *Fistulina hepatica* (Fistulinaceae). The gene repertoire of *A. ampla* (15,576 genes) is very similar
111 to that of *S. commune* [2](16,319 genes) and the average gene count in the analyzed Agaricales
112 species (17,655), but more than that of *F. hepatica* [9] (11,244 genes). We found 8 significantly
113 overrepresented (p-value<=0.05) and 16 underrepresented (p-value<=0.05) InterPro domains in
114 both species, relative to the other 29 species (Supplementary Table 1).

Auriculariopsis and *Schizophyllum* have unusual wood-decay strategies

The substrate-wise phylogenetic PCA portrays a separation of these two species from the other 29 species used in this dataset. In the case of cellulases, these two species cluster together with WRs and S/L/O, suggesting a similar arsenal of CAZymes acting on the cellulose degradation (Figure 1b). Enzyme families acting on crystalline cellulose (cellobiohydrolases - GH6, GH7) were present in lower numbers than in WRs and S/L/O species, but similar to ectomycorrhizal ones. The pattern was mostly identical for hemicellulases and pectinases (Figure 1b) where CAZyme copy numbers were similar to that of white rotters and litter decomposers. However, some CAZymes related to xylanase and pectinase activities including xylosidases, pectate lyases, pectin acetylesterases, and acetyl xylan esterases (AA8, GH30, GH43, GH95, CE12, PL1, PL3, PL4) have higher copy numbers in the two species than in most WRs. This could imply their role in hemicellulose and pectin degradation, as reported previously [10]. However, ligninolytic CAZymes revealed a clear difference from WR species. The absence of class II peroxidases in both species [6–8] , made them cluster towards ectomycorrhizal and BR species. Copper radical oxidases (CROs) are known to be responsible for the production hydrogen peroxide and were also reported to have a significantly different repertoires in BRs and WRs [9]. In our analysis we found very low numbers of CROs (AA5) in *Auriculariopsis* and *Schizophyllum* as compared to ECM, S/L/O and WR species.

Because *A. ampla* and *S. commune* often occur on bark as first colonizers, we also examined protein families that putatively degrade important bark compounds. Suberin, lignin and tannins represent the major components of bark [38–40]. We built on previous datasets to obtain putative suberinase [38,39] and tannase [40] copy numbers for 31 species in our dataset. In general, suberin comprises aromatic compounds cross linked by poly-aliphatic and fatty-acid like components which requires extracellular esterases and lipases for their breakdown [38]. Based on

phylogenetic PCA of putative suberinases *A. ampla* and *S. commune* were transitional between typical WR and ECM, BR (*Fistulina*), uncertain (*Cylindrobasidium, Pluteus)* or tentative WR (*Fibulorhizoctonia*) species. This separation is most pronounced along the first axis (PC1), the main contributor of which is the AA3 family. *A. ampla* and *S. commune* had few genes in this family, similar to most ECM species. In terms of most other families, *A. ampla* and *S. commune* resembled WR species. The cutinase (CE5) repertoires of the two species are similar to those of litter decomposers and certain WR taxa (e.g. *Galerina, Dendrothele, Fibulorhizoctonia,* and *Peniophora*), although this family was missing from several WR species. Tannin acyl hydrolases (tannase, EC 3.1.1.20) are responsible for the degradation of tannins, polyphenolic plant secondary metabolites characteristic to the bark and wood tissues. Tannases were found in 10 out of 31 species, mostly in those that occur preferentially on bark, such as *Auriculariopsis, Schizophyllum, Peniophora*, *Dendrothele* and *Plicaturopsis,* and a few others *(Gymnopus, Pterula, Fibulorhizoctonia, Omphalotus* and *Fistulina*). This could indicate a specialization of these species to substrates with high tannin content, such as bark, suggesting adaptations to the early colonization of bark-covered wood. Notably, *Pluteus*, a species with an uncertain nutritional mode, groups closely together with *A. ampla* and *S. commune* on the suberinase PCA, although it had low pectinase, hemicellulase and cellulase copy numbers, leading to a position close to ECM species and some litter decomposers in other PCA analyses (Supplementary Figure 1).

Transcriptomics reveals a high rate of developmental evolution

Auriculariopsis ampla and *S. commune* have a similar developmental progression (Figure 2a-2e), permitting a comparison of their transcriptional programs. Fruiting body development starts in both species with the appearance of minute globose primordia (stage 1 primordia), in which a cavity develops (Stage 2 primordia). This cavity further expands in *A. ampla* to produce an open,

163 pendant fruiting body (Young fruiting body and fruiting body stages), whereas in *S. commune*
164 several such units form a multi-lobed assemblage.

165 For comparison with *S. commune*, we generated RNA-Seq data from 5 developmental
166 stages of *A. ampla* (vegetative mycelium, stage 1 and stage 2 primordia, young and mature
167 fruiting bodies, see Figure 2a-b,d) in biological triplicates, >30 million (30-78M, mean: 46M)
168 paired-end 150 base reads for each sample on Illumina platform (mean read mapping: 83%,
169 Supplementary Table 2). Corresponding data for the same developmental stages (Figure 2c, e)
170 for *S. commune* were taken from (ref. 3). Based on global transcriptome similarity, fruiting body
171 samples grouped together away from vegetative mycelium ones (Figure 3a) consistent with the
172 complex multicellular nature of fruiting bodies as opposed to a simpler cellularity level of
173 vegetative mycelia. Among the fruiting body samples, stage 1 and stage 2 primordia were similar
174 to each other, whereas young fruiting bodies and mature fruiting bodies formed distinct groups.
175 We identified 1466 developmentally regulated genes in *A. ampla*, which is similar in magnitude
176 to that reported for *S. commune*, but less than that for more complex species (e.g. *Coprinopsis*,
177 *Armillaria*; taken from (ref. 3). Of the developmentally regulated genes, 967 showed a
178 significant (≥4) fold change in the transition from vegetative mycelium to stage 1 primordia. In
179 terms of significantly differentially expressed genes (DEGs), the highest numbers of up and
180 downregulated were also found between vegetative mycelium and stage 1 primordia (1166 and
181 842 genes, Figure 3b), which is consistent with the position of samples on the MDS plot (Figure
182 3a). Much fewer genes were differentially expressed between stage 1 and 2 primordia and
183 between stage 2 primordia and young fruiting bodies. In fruiting bodies, we found 110 and 37
184 significantly up- and downregulated genes, respectively, a comparatively higher number that is
185 potentially related to sporulation.

We assessed the similarity between the 2 species' developmental transcriptomes by analyzing the expression of one-to-one orthologous gene pairs, hereafter referred to as co-orthologs. To identify co-orthologs, proteomes of *A. ampla* and *S. commune* were clustered into 18,804 orthogroups using MCL, of which 7463 represented co-orthologs. Of these, 7369 co-orthologs were expressed under our experimental conditions in both species (Supplementary Table 3). Pairwise comparison between developmental stages showed highest similarity within species across all 7369 co-orthologs (Figure 4a). This pattern was more pronounced in an analysis of developmentally regulated co-orthologs (Figure 4b, see Methods), indicating that developmental gene expression in *A. ampla* and *S. commune* has diverged since their common ancestor so that similarity between homologous fruiting body stages of the two species is lower than that between different stages of the same species. Vegetative mycelia of both species differed most from all other stages of the same species but showed some similarity across species. Similarly, we observed a strong similarity between young fruiting bodies and fruiting bodies of *A. ampla* and *S. commune*, indicating that late stages of fruiting body development share more similarity across species than do early stages. Similar patterns were observed when the analyses were restricted to co-orthologous transcription factors (Figure 4c) and its developmentally regulated subset (Figure 4d). Similarity between late developmental stages of the two species was more pronounced in the analysis of developmentally regulated genes. Given that *A. ampla* and *S. commune* are each other's closest relatives, the low similarity of gene expression among their fruiting bodies (Figure 4) indicates that developmental gene expression has diverged at a high speed since their divergence. This is surprising in comparison to similar analyses of animals, where gene expression patterns could be predicted from tissue identities across the entire mammalian clade [41]. This suggests that fruiting body development evolved at a high rate, erasing identities of similar developmental stages across species. Nevertheless, these

data show that during fruiting body maturation gene expression dynamics shows conserved patterns among phylogenetically closely related species. These data further indicate that there should be genes with similar expression profiles in *A. ampla* and *S. commune*.

Despite the low global similarity, several genes with conserved expression patterns could be identified. The most highly upregulated co-ortholog in *A. ampla* and *S. commune* was a heat shock protein 9/12 family member, that is homologous to *Aspergillus nidulans* awh11 and *S. cerevisiae* hsp12, farnesol-responsive heat shock proteins. These genes had a significant upregulation in stage 1 primordia of both *A. ampla* and *S. commune* (fold change 254x and 855x, respectively) and had high expression values in all fruiting body tissues (>5,000 FPKM, maximum fold change within fruiting bodies 3.4-3.7), suggesting an important role of heat shock proteins during fruiting body development. In further support of this hypothesis, homologs of these genes were found developmentally regulated or differentially expressed also in *Laccaria bicolor* [21], *Lentinula edodes* [42], *Armillaria ostoyae, Coprinopsis cinerea, Lentinus tigrinus,* and *Rickenella mellea* [3]. Another co-orthogroup with large upregulation in stage 1 primordia included A1 aspartic proteases, although the expression dynamics were somewhat different in the two species. We observed an induction in stage 1 primordia in both, but, while upregulation in *A. ampla* was >200x compared to VM, it was only 14x in *S. commune*. Aspartic proteases of the diverse A1 family have been reported as highly induced in fruiting bodies in several previous studies [3,21,42–44], although no mechanistic hypothesis for their role in fruiting body development has been proposed yet.

Putative fruiting body genes are developmentally expressed

We further examined the expression patterns of previously reported fruiting body genes in *A. ampla*. Of the fungal cell wall (FCW) associated genes, hydrophobins were mostly developmentally regulated (8 out of 11 genes) in *A. ampla* (Supplementary Figure 2), often with

234 significantly increased expression coincident with the transition from vegetative mycelium to
235 stage 1 primordia (in six genes), as observed previously [1,42,45–47]. Several members of two
236 functionally similar families, cerato-platanins (4 of 5 genes dev. reg.) and expansin-like genes
237 (10 of 21 genes) were likewise developmentally regulated. Although cerato-platanins and
238 expansins were often associated with the plant cell wall [48,49], their dynamic expression in fruiting
239 bodies suggest potential FCW-related roles. Functional annotations uncovered several putatively
240 FCW-active CAZymes (Supplementary Figure 3), including chitin- and glucan- active GH and
241 GT families, carbohydrate-binding modules, carbohydrate esterases, AA1 multicopper oxidases,
242 AA9 lytic polysaccharide monooxygenases, but also starch synthesizing glycosyl transferases
243 (e.g. GH15, CBM20), which might be related to the mobilization of glycogen reserves during
244 development. Two out of 10 members of the Kre9/Knh1 family were developmentally regulated.
245 This family is involved in *β*-1,6-glucan synthesis and remodeling in *Aspergillus fumigatus* [50],
246 *Candida albicans* [51], *Saccharomyces cerevisiae* [52] and *Ustilago maydis* [53] and has been shown to
247 be developmentally expressed in Agaricomycetes fruiting bodies [3,54]. Its widespread FCW-
248 associated role in both Asco- and Basidiomycota suggests a plesiomorphic role in *β*-glucan
249 assembly in the cell wall and suggests that this family has been co-opted for fruiting body
250 development in Agaricomycetes. Several other previously reported putatively FCW-active
251 CAZyme families [3,21,42,55–58] (e.g GH5, GH142 [5,59–61], Supplementary Figure 2), also showed
252 developmental expression in *A. ampla*, reinforcing the view that cell wall remodeling is a
253 fundamental mechanism in fruiting body development [2,3,5,21,31,58,62–64].

254 Defense related genes have been in the focus of research on fruiting bodies. We found
255 developmentally regulation of a diverse array of putative defense-related genes by searching for
256 homologs of *Coprinopsis* defense genes [65]. *A. ampla* and *S. commune* have reduced repertoires of
257 defense-related genes compared to *Coprinopsis cinerea* (Supplementary Figure 2). For example,

no homologs of aegerolysins or the ETX/MTX2 pore forming toxin family have been found in their genomes, whereas lectins are only represented by 14 genes as opposed to 39 and 25 in *C. cinerea* and *A. ostoyae*. They have several genes in the thaumatin family, with has been associated with defense [65] in both fungi and plants [66,67], fungal pathogenicity [68] but also with FCW remodeling [62,69], depending on the scope of the study. Based on its endo-β-1,3-glucanase activity, its efficiency in degrading cell wall components of *Lentinula edodes* [62] and *Saccharomyces* [69] and developmental expression in axenic fruiting bodies, it appears likely that members of this family are involved in FCW remodeling, although antimicrobial activities have also been predicted for certain members [3]. Cerato-platanins represent a similar case. This is a family widely expressed in pathogenic fungal-plant interactions [70,71], fruiting bodies [3,4,71] and defense assays [65] and significantly enriched in Agaricomycetes genomes [3,70]. We detected four developmentally regulated cerato-platanin genes in *A. ampla*, three of which showed an induction at the transition from vegetative mycelium to stage 1 primordia (Supplementary Figure 2). *S. commune* had three developmentally regulated cerato-platanins, with non-matching expression profiles. Further, in *A. ampla* we found 3 developmentally regulated lectin genes (Supplementary Figure 2), as opposed to *S. commune*, which had 8 [3]. All three genes belong to the ricin-B lectin family and harbor a CBM13 domain, which has demonstrated mannose, N-acetylgalactosamine and xylane binding activities [72,73]. Ricin-B lectins have been reported as developmentally expressed in fruiting bodies of all Agaricomycetes tested so far [3,4,28,42,57,65], although its functions are less clear. It is the largest family of basidiomycete lectins [3] and was shown to be toxic to nematodes [29,74], although their diverse carbohydrate-binding abilities (mannose and N-acetylgalactosamine) could confer additional or other functions as well.

F-box and BTB/POZ domain containing proteins have recently been reported as an interesting family with probable functions in fruiting body development and a significant

expansion in the Agaricomycetes [3]. *Auriculariopsis* has 246 F-box protein encoding genes, of which 12 were developmentally regulated in our dataset. Of the 96 BTB/POZ domain-containing proteins 26 were developmentally regulated, including some genes with remarkable expression dynamics during development (e.g. fold change 526x, Auramp1_515369). This is similar to figures reported for *S. commune* [3]. These domains are involved in protein-protein interactions and have been reported to act as transcriptional repressors [75], members of selective proteolysis pathways, and include homologs of yeast *Skp1* [76] too. Although very little functional information on these families is available in fungi, their expression dynamics in development and previously reported regulatory roles suggest they could be important players in fruiting body development.

Conserved patterns of transcription factors expression

We examined expression patterns of transcription factors (TFs) and their similarity between the two species. We identified 433 and 437 TFs in the genomes of *A. ampla* and *S. commune* respectively, of which 252 were co-orthologs. These were distributed across 28 TF families, with C2H2-type Zinc finger and Zn (2)-C6 fungal-type TFs being the most dominant (Supplementary Table 4). Individually, 14,5% and 16% of the *Auriculariopsis* and *Schizophyllum* and 17% of the co-orthologous TFs were developmentally regulated, respectively.

These included 5 of the eight previously characterized TF genes of *S. commune* [1]: *c2h2, gat1, hom1, tea1* and *fst4* showed significant changes in expression, in most cases at the initiation of fruiting body development, whereas *fst3, bri1* and *hom2* showed more or less flat expression profiles (Figure 5). These expression profiles are consistent with previous RNA-Seq based reports [24] in *Schizophyllum* and other species [65,77–79], except in *hom1* and *gat1*, which, in our data behaved differently, probably due to the different resolution of developmental stage data. The expression profiles of all eight genes were very similar between *A. ampla* and *S. commune*. Homologs of *Lentinula edodes PriB* [80,81] (Auramp1_518770, Schco3_2525437) were

306 also developmentally regulated, with an expression peak in stage 1 primordia. Homologues of
307 *Coprinopsis exp1*, which was reported to be involved in cap expansion [82], were present in both
308 species and had a matching expression profile, but were not developmentally regulated in our
309 data. In our experiments, *exp1* homologs (Auramp1_481073, Schco3_2623333) showed highest
310 expression in vegetative mycelia and lower expression afterwards, which might be related to the
311 lack of proper caps in *A. ampla* and *S. commune*.

312 Of the 252 co-orthologous TFs, 42 were developmentally regulated in both species, 27 of
313 which had similar expression profiles between *A. ampla* and *S. commune*. Nine of the most
314 interesting of these TFs are shown on Figure 5. Three of these genes showed highest expression
315 in vegetative mycelia and are probably not relevant to fruiting body development. For the other
316 six genes an upregulation was observed at the transition from vegetative mycelia to stage 1
317 primordia, which is compatible with potential roles in the initiation of fruiting body development
318 or accompanying morphogenetic changes. Such TFs, with conserved, developmentally dynamic
319 expression might be related to sculpting the specialized, cyphelloids fruiting body morphologies
320 of *Auriculariopsis* and *Schizophyllum* or more widely conserved fruiting body functions. This
321 also shows the power of comparative transcriptomics to identify genes with conserved
322 expression patterns during fruiting body development [83] and to generate hypotheses that are
323 testable by gene knockouts or functional assays.

324 Small secreted proteins show dynamic expression in fruiting bodies

325 We detected several genes encoding short proteins with extracellular secretion signals (SSPs) in
326 the fruiting body transcriptomes. In *A. ampla* and *S. commune* 316 and 354 SSPs were detected,
327 respectively, half of which contained no known InterPro domains (Figure 6a, Supplementary
328 Table 6). The SSPs in the two species belonged to 283 orthologs in *A. ampla*, and 315 in *S.*
329 *commune*. Out of these, 133 orthologs were shared by the two species, whereas 150 and 182

were specific to *A. ampla* and *S. commune,* respectively (Figure 6b). The 133 shared orthologs contained 162 proteins, of which 39 were developmentally regulated in *A. ampla* and 158, with 54 developmentally regulated in *S. commune*. From these, 20 orthologs were developmentally regulated in both species (Figure 6d) and had a similar expression profile. Annotated SSPs in the two species (Figure 6c) had similar expression dynamics and mainly comprised hydrophobins, ceratoplatanins, CFEM domain containing proteins, concanavalin type lectins, and glycosyl hydrolases [3]. The 150 species specific orthogroups in *A. ampla* contained 154 proteins, of which 32 are developmentally regulated. The 182 orthogroups in *S. commune* contained 196 proteins, of which 58 are developmentally regulated (Supplementary Figure 4).

We detected several developmentally regulated SSP-s with no annotations, some of which showed high expression dynamics (FC>50, Figure 6e). We found 8, 15 and 2, *Auriculariopsis*-specific, *Schizophyllum*-specific and shared SSPs, respectively, with no known domains but a high expression dynamics (Supplementary Figure 4, Supplementary Table 6). For example, one of the orthogroups (Auramp1_494084, Auramp1_549528, Schco3_2664662) showed a considerable upregulation in stage 1 primordia in both species (FC=1166 - 1870), suggesting a role in the transition from vegetative mycelium to fruiting body initials. Such SSPs resemble effector proteins involved in cell-to-cell communication in ectomycorrhizal and pathogenic interactions between fungi and plants [84,85]. Their expression in fruiting bodies raises the possibility that they play signaling roles and may be responsible for sculpting the fruiting bodies of these fungi. SSPs with an upregulation in morphogenetic processes (ECM root tips and/or fruiting bodies) have been reported in *Laccaria* [21,84,86] and *Pleurotus* [87] suggesting a role in tissue differentiation and that some of the SSPs initially found in ECM root tips may actually be morphogenetic in nature. Whether morphogenesis-related SSPs occur ubiquitously among mushroom-forming fungi and what is the mechanistic basis of their role, needs further research.

Conclusions

In this study we presented the genome sequence of *Auriculariopsis ampla* and performed comparative genomic and transcriptomic analyses with *Schizophyllum commune* and other Agaricomycetes, to identify conserved genes related to fruiting body development and wood-decay. Our results showed that the two analyzed members of the Schizophyllaceae have a potential to shape our understanding of Agaricomycete biology. The CAZyme composition of *A. ampla* and *S. commune* compared to other 29 species suggests that the wood degrading strategies of the two species show similarity to WRs when concerned with cellulases, hemicellulases, and pectinolytic gene families. What sets them apart from WRs is the absence of class II PODs, which is also the case for BRs and ectomycorrhizal fungi. However, the reduction in ligninolytic genes is compensated by the presence of suberinases and tannases required to depolymerize important components bark, to which these species might be adapted.

Our analyses revealed a large number of genes with developmentally dynamic expression in fruiting bodies of both *A. ampla* and *S. commune*, including transcription factors (including 9 new conserved TFs), carbohydrate-active enzymes, heat shock proteins, aspartic proteases, as well as small secreted proteins. Particularly interesting are SSP-s with a highly dynamic expression through development, due to the role of SSPs in intracellular communication in pathogenic and ectomycorrhizal associations [84,85]. Although mechanistic evidence is still lacking, it is conceivable that SSP-s with fruiting body specific expression might be involved in intercellular communication in fruiting bodies, similarly to their mycorrhiza and pathogenicity-related counterparts. This hypothesis would provide an explanation for the rich SSPs content of fruiting-body forming Agaricomycetes that are neither ectomycorrhizal or pathogenic [3,84].

Our data also suggest that despite the close phylogenetic relatedness of *Auriculariopsis* and *Schizophyllum*, their developmental transcriptomes have diverged significantly since their

common ancestors, indicating a high rate of developmental gene expression in these taxa. Such divergence might be related to morphogenetic differences between the two species: while *A. ampla* produces simple cyphelloid (cup-shaped) fruiting bodies, those of *S. commune* consist of several congregated cyphelloid modules. Despite this divergence, several genes with a matching expression profile could be identified, highlighting conserved roles that await further experimentation. These data have the potential to highlight not only the genes involved in the development of cyphelloid fruiting bodies, but also that of other agaricomycete fruiting body types and as such, should be immensely useful to understanding the general principles and shared properties of fruiting body development in mushroom-forming fungi.

Acknowledgements

This work was supported by the 'Momentum' program of the Hungarian Academy of Sciences (Contract No. LP2014/12 to L.G.N.) and the European Research Council (Grant No. 758161 to L.G.N.). The work conducted by the U.S. Department of Energy Joint Genome Institute (JGI), a DOE Office of Science User Facility, was supported by the Office of Science of the U.S. Department of Energy under Contract No. DE-AC02-05CH11231. This work was supported by the National Research, Development and Innovation office (Contract No. Ginop-2.3.2-15-00002, to L.G.N.).

Methods

Genome sequencing

The sequenced strain of *Auriculariopsis ampla* was collected as fruiting bodies on the bark of in Szeged, Hungary and cultured in liquid malt-extract medium (deposited in Szeged

Microbiological Collections, under NL-1724). DNA was extracted using the DNeasy Blood & Tissue Culture kit (Qiagen), following the manufacturer's protocol. The genome was sequenced using Pacific Biosciences RS II platform. Unamplified libraries were generated using Pacific Biosciences standard template preparation protocol for creating >10kb libraries. 5 ug of gDNA was used to generate each library and the DNA was sheared using Covaris g-Tubes (TM) to generate sheared fragments of >10kb in length. The sheared DNA fragments were then prepared using Pacific Biosciences SMRTbell template preparation kit, where the fragments were treated with DNA damage repair, had their ends repaired so that they were blunt-ended, and 5' phosphorylated. Pacific Biosciences hairpin adapters were then ligated to the fragments to create the SMRTbell template for sequencing. The SMRTbell templates were then purified using exonuclease treatments and size-selected using AMPure PB beads. Sequencing primer was then annealed to the SMRTbell templates and Version P6 sequencing polymerase was bound to them. The prepared SMRTbell template libraries were then sequenced on a Pacific Biosciences RSII sequencer using Version C4 chemistry and 4-hour sequencing movie run times. Filtered subread data was assembled together with Falcon version 0.4.2 (https://github.com/PacificBiosciences/FALCON) and subsequently polished with Quiver version smrtanalysis_2.3.0. 140936.p5 (https://github.com/PacificBiosciences/GenomicConsensus).

For transcriptome, Stranded cDNA libraries were generated using the Illumina Truseq Stranded RNA LT kit. mRNA was purified from 1 ug of total RNA using magnetic beads containing poly-T oligos. mRNA was fragmented and reversed transcribed using random hexamers and SSII (Invitrogen) followed by second strand synthesis. The fragmented cDNA was treated with end-pair, A-tailing, adapter ligation, and 8 cycles of PCR. The prepared library was quantified using KAPA Biosystem's next-generation sequencing library qPCR kit and run on a

Roche LightCycler 480 real-time PCR instrument. The quantified library was then multiplexed with other libraries, and the pool of libraries prepared for sequencing on the Illumina HiSeq sequencing platform utilizing a TruSeq paired-end cluster kit, v4, and Illumina's cBot instrument to generate a clustered flow cell for sequencing. Sequencing of the flow cell was performed on the Illumina HiSeq2500 sequencer using HiSeq TruSeq SBS sequencing kits, v4, following a 2x150 indexed run recipe. Illumina fastq files were QC filtered for artifact/process contamination and de novo assembled with Trinity v2.1.1 [88] and used for genome annotation

The genome was annotated using the JGI Annotation pipeline [89] and made available via JGI fungal genome portal MycoCosm (jgi.doe.gov/fungi;[89]). The data also deposited at DDBJ/EMBL/GenBank under the accession *(TO BE PROVIDED UPON PUBLICATION).*

Fruiting protocol, RNA extraction and transcriptome sequencing

Fruiting and RNA extraction

Auriculariopsis ampla was grown on sterilized poplar (*Populus alba*) bark and wood plugged into malt-extract medium in 250 ml glass beakers. Cultures were pre-incubated for 14 days in the dark at 30°C, then transferred to room temperature 60 cm under a light panel of 6 Sylvania Activa 172 Daylight tubes, with a 12 hr light/dark cycle and >90% relative humidity. Primordia started to develop 7 days after the transfer to light.

Vegetative mycelium, Stage 1 and 2 primordia, young and mature fruiting bodies were collected with sterilized forceps, flash-frozen in liquid nitrogen and stored at -80°C. Stage 1 and 2 primordia were defined as 0.1-1 mm closed, globular structures and 1-2 mm long initials with a central externally visible pit, respectively. We considered already opened fruiting bodies with a cup shape, 3-6 mm wide as young fruiting bodies and fully open ones as mature fruiting bodies. Total RNA was extracted from tissues ground to a fine powder in a mortar, using the Quick-

RNA Miniprep kit (Zymo Research), following the manufacturer's protocol. RNA samples with RIN>8 was saved for RNA-Sequencing. For each sample type three biological replicates were processed.

RNA-Seq

Whole transcriptome sequencing was performed using the TrueSeq RNA Library Preparation Kit v2 (Illumina) according to the manufacturer's instructions. RNA quality and quantity were assessed using RNA ScreenTape and Reagents on TapeStation (all from Agilent) and Qubit (ThermoFisher); only high quality (RIN >8.0) total RNA samples were processed. Next, RNA was DNaseI (ThermoFisher) treated and the mRNA was purified based on PolyA selection and fragmented. First strand cDNA synthesis was performed using SuperScript II (ThermoFisher) followed by second strand cDNA synthesis, end repair, 3'-end adenylation, adapter ligation and PCR amplification. Purification steps were performed using AmPureXP Beads (Backman Coulter). Final libraries were quality checked using TapeStation. Concentration of each library was determined using either the qPCR Quantification Kit for Illumina (Agilent) or the KAPA Library Quantification Kit for Illumina (KAPA Biosystems). Sequencing was performed on Illumina instruments using the HiSeq SBS Kit v4 250 cycles kit (Illumina) generating >20 million clusters for each sample.

Bioinformatic analyses of RNA-Seq data

RNA-Seq analyses were carried out as reported earlier [3,4]. Paired-end Illumina (HiSeq) reads were quality trimmed using CLC Genomics Workbench 9.5.2 (CLC Bio/Qiagen), removing ambiguous nucleotides as well as any low quality read ends. Quality cutoff value (error probability) was set to 0.05, corresponding to a Phred score of 13. Trimmed reads containing at

least 40 bases were mapped using the RNA-Seq Analysis 2.1 package in CLC requiring at least 80% sequence identity over at least 80% of the read lengths; strand specificity was omitted. Reads with less than 30 equally scoring mapping positions were mapped to all possible locations while reads with more than 30 potential mapping positions were considered as uninformative repeat reads and were removed from the analysis.

"Total gene read" RNA-Seq count data was imported from CLC into R 3.0.2. Genes were filtered based on their expression levels keeping only those features that were detected by at least five mapped reads in at least 25% of the samples included in the study. Subsequently, "calcNormFactors" from "edgeR" 3.4.2 [90] was used to perform data scaling based on the "trimmed mean of M-values" (TMM) method73. Log transformation was carried out by the "voom" function of the "limma" package 3.18.13 [91]. Linear modeling, empirical Bayes moderation as well as the calculation of differentially expressed genes were carried out using "limma". Genes showing at least four-fold gene expression change with an FDR value below 0.05 were considered as significantly differentially expressed. Multi-dimensional scaling ("plotMDS" function in edgeR) was applied to visually summarize gene expression profiles revealing similarities between samples.

Developmentally regulated genes were defined as genes showing an >4-fold change in expression through development. In comparisons of vegetative mycelia and stage 1 primordia, we only considered genes upregulated in primordia, to exclude genes that showed a highest expression in vegetative mycelium because those might be related to processes not relevant for fruiting body development (e.g. nutrient acquisition).

Phylogenetic analysis

Single-copy orthogroups were identified in MCL clusters of the 31 Agaricomycetes and were aligned by the l-ins-i algorithm of MAFFT [92]. Ambiguously aligned regions were removed using

497 the 'strict' settings of Trim-Al. Trimmed alignments longer than 100 amino acids were
498 concatenated into a supermatrix. A maximum likelihood phylogenetic analysis was performed in
499 RAxML 8.2.11 under the PROTGAMMALG model, with a gamma-distributed rate
500 heterogeneity and a partitioned model. A bootstrap analysis in 100 replicates was performed.

501 Identification of orthologous groups and their functional annotations

502 Groups of orthologous genes have been identified using OrthFinder v 1.1.8 [93], based on predicted
503 protein sequences and the program's default parameters. Two analyses were performed, one to
504 delimit orthogroups across 31 Agaricomycetes species and the second to find co-orthologs
505 shared by *A. ampla* and *S. commune*, both using identical parameters. Functional annotation of
506 proteins was carried out based on InterPro domains using InterProscan version 5.28-67.0 across
507 the 31 fungal proteomes.

508 Analyses of Carbohydrate Active Enzymes (CAZymes)

509 The CAZymes in the 31 species used in this study were annotated using the CAZy annotation
510 pipeline [94]. Copy numbers for most species were extracted from JGI Mycocosm, whereas those
511 of *Flammulina velutipes, Coprinopsis marcescibilis,* and *Galerina marginata* were annotated for
512 this study. Of all the families found in the dataset, we took into account the CAZyme families
513 reported having a putative role in plant cell wall degradation [6,8,9,22](Supplementary Table 5) and
514 analyzed their copy numbers across the 31 species. We used 45 CAZy families in our dataset
515 (Supplementary Table 5) and divided them based on the degradation of celluloses,
516 hemicelluloses, lignin, pectin.

517 In addition to these substrates, we also assessed genes encoding proteins with putative
518 roles in suberin and tannin degradation. We extracted the best BLAST hits (BLAST 2.7.1+, e-
519 value 0.001) from the 31 species for the homologs of proteins suggested to be related to suberin
520 [38,39] and tannin degradation [40]. We then identified the orthoMCL clusters of the 31 species

containing the best hits. The proteins belonging to these clusters were used for further analysis as putative suberinases or tannases (Supplementary Table 5).

In order to get insights into the nutritional strategies employed by *A. ampla* and *S. commune*, we compared copy numbers of these species to that of 29 Agaricomycetes species with one of five known nutritional modes: brown rotters (BR), ectomycorrhizal (ECM), saprotrophs/litter decomposers/organic matter degraders (S/L/O), white rotters (WR) and uncertain. To analyze the grouping of the species according to their substrate degradation capabilities, phylogenetic PCA was performed using the phyl.pca [95] function from the R package phytools [96]. A matrix of gene number normalized by proteome size in each organism (Supplementary Table 5), and the ML species tree, were used as input. Independent contrasts were calculated under the Brownian motion model and the parameter mode="cov".

Analyses of transcriptome similarity

Pairwise comparisons of *A. ampla* and *S. commune* transcripts based on Pearson correlation coefficient among all replicates and developmental stages of 7369 OGs and among 1182 OGs containing at least one developmentally regulated gene were performed using custom Python script (pandas v 0.18.1 and Matplotlib v. 1.1.1 libraries). The same analysis has been performed for 252 single-copy ortholog transcription factors. The resulting matrix of Pearson correlation coefficients was plotted as a heatmap using the Matplotlib v. 1.1.1 pyplot framework. A scatterplot was constructed based on the log fold changes (FCs) of co-orthologs in *A. ampla* and *S. commune* using the 'ggplot' R package.

Heatmaps were created for developmentally regulated genes using the heatmap.2 function of R 'gplot' package. Hierarchical clustering with Euclidean distance calculation and averaged-linkage clustering was carried out on the FPKM values using 'hclust' function in R,

and heatmaps was visualized using z-score normalization on the rows via the heatmap.2 function.

Identification of transcription factors and other fruiting body genes

We identified transcription factor encoding genes in the proteomes of 31 Agaricomycetes species based on InterPro annotations. Only proteins containing domains with sequence-specific DNA binding ability were considered as transcription factors [3].

Carbohydrate active proteins were identified through the CAZy pipeline as described above.

We extracted the kinases of the 2 species based on their InterPro domain composition and eliminated the ones involved in metabolism. Based on BLAST (*v*2.7.1+, e-value 0.001) against the classified kinome of *Coprinopsis cinerea* (Kinbase, Stajich et al., 2010), we assigned the best hits into the kinase categories of the query protein ([97,98]; www.kinase.com). Heatmaps were created using the Heatmap.2 function in R and are based on the FPKM values of developmentally regulated genes.

Analyses of small secreted proteins

Small Secreted Proteins (SSPs) were identified for the two species to grasp species-specific and conserved SSPs in the two species. SSPs were defined as proteins shorter than 300 amino acids, having a signal peptide, an extracellular localization and no transmembrane domain. Proteins shorter than 300 amino acids were subjected to signal peptide prediction through SignalP 4.1[99] with the option "eukaryotic". The proteins having extracellular signal peptide were checked for their extracellular localization using WoLF PSORT 0.2 [100] with the option "fungi" and these were further checked for the absence of transmembrane helices, using TMHMM 2.0 [101].

References

1. Ohm RA, de Jong JF, de Bekker C, Wösten HAB, Lugones LG. Transcription factor genes of Schizophyllum commune involved in regulation of mushroom formation. Mol Microbiol. 2011;81(6):1433–45.

2. Ohm RA, De Jong JF, Lugones LG, Aerts A, Kothe E, Stajich JE, et al. Genome sequence of the model mushroom Schizophyllum commune. Nat Biotechnol. 2010;28(9):957–63.

3. Krizsan K, Almasi E, Merenyi Z, Sahu N, Viragh M, Koszo T, et al. Transcriptomic atlas of mushroom development highlights an independent origin of complex multicellularity. bioRxiv. 2018 Jun;349894.

4. Sipos G, Prasanna AN, Walter MC, O'Connor E, Bálint B, Krizsán K, et al. Genome expansion and lineage-specific genetic innovations in the forest pathogenic fungi Armillaria. Nat Ecol Evol. 2017 Dec;1(12):1931–41.

5. Sakamoto Y, Nakade K, Konno N. Endo-β-1,3-Glucanase GLU1, from the fruiting body of Lentinula edodes, belongs to a new glycoside hydrolase family. Appl Environ Microbiol. 2011;77(23):8350–4.

6. Floudas D, Binder M, Riley R, Barry K, Blanchette RA, Henrissat B, et al. The Paleozoic Origin of Enzymatic Lignin Decomposition Reconstructed from 31 Fungal Genomes. Science. 2012 Jun 29;336(6089):1715–9.

7. Martinez D, Challacombe J, Morgenstern I, Hibbett D, Schmoll M, Kubicek CP, et al. Genome, transcriptome, and secretome analysis of wood decay fungus *Postia*

*placenta*supports unique mechanisms of lignocellulose conversion. Proc Natl Acad Sci. 2009;106(6):1954–9.

8. Riley R, Salamov AA, Brown DW, Nagy LG, Floudas D, Held BW, et al. Extensive sampling of basidiomycete genomes demonstrates inadequacy of the white-rot/brown-rot paradigm for wood decay fungi. Proc Natl Acad Sci U S A. 2014 Jul;111(27):9923–8.

9. Floudas D, Held BW, Riley R, Nagy LG, Koehler G, Ransdell AS, et al. Evolution of novel wood decay mechanisms in Agaricales revealed by the genome sequences of Fistulina hepatica and Cylindrobasidium torrendii. Fungal Genet Biol. 2015;76:78–92.

10. Zhu N, Liu J, Yang J, Lin Y, Yang Y, Ji L, et al. Comparative analysis of the secretomes of Schizophyllum commune and other wood-decay basidiomycetes during solid-state fermentation reveals its unique lignocellulose-degrading enzyme system. Biotechnol Biofuels [Internet]. 2016 Dec [cited 2019 Feb 3];9(1). Available from: http://www.biotechnologyforbiofuels.com/content/9/1/42

11. Schmidt O, Liese W. Variability of Wood Degrading Enzymes of *Schizophyllum commune*. Holzforschung. 1980 Jan;34(2):67–72.

12. Padhiar A, Albert S. Anatomical changes in Syzygium cumuini Linn. wood decayed by two white rot fungi Schizophyllum commune Fries. and Flavodon flavus (Klotzsch) Ryvarden. J Indian Acad Wood Sci. 2011 Jun;8(1):11–20.

13. Schmidt O, Liese W. Variability of Wood Degrading Enzymes of *Schizophyllum commune*. Holzforschung. 1980 Jan;34(2):67–72.

606 14. Takemoto S, Nakamura H, Imamura Y, Shimane T. Schizophyllum commune as a
607 Ubiquitous Plant Parasite. Jpn Agric Res Q JARQ. 2010;44(4):357–64.

608 15. Kües U, Navarro-González M. How do Agaricomycetes shape their fruiting bodies? 1.
609 Morphological aspects of development. Vol. 29, Fungal Biology Reviews. 2015. p. 63–97.

610 16. Kües U, Liu Y. Fruiting body production in basidiomycetes. Appl Microbiol Biotechnol.
611 2000 Aug 15;54(2):141–52.

612 17. Sakamoto Y, Sato S, Ito M, Ando Y, Nakahori K, Muraguchi H. Blue light exposure and
613 nutrient conditions influence the expression of genes involved in simultaneous hyphal knot
614 formation in Coprinopsis cinerea. Microbiol Res. 2018 Dec;217:81–90.

615 18. Muraguchi H, Umezawa K, Niikura M, Yoshida M, Kozaki T, Ishii K, et al. Strand-specific
616 RNA-seq analyses of fruiting body development in Coprinopsis cinerea. PLoS ONE.
617 2015;10(10).

618 19. Stajich JE, Wilke SK, Ahren D, Au CH, Birren BW, Borodovsky M, et al. Insights into
619 evolution of multicellular fungi from the assembled chromosomes of the mushroom
620 Coprinopsis cinerea (Coprinus cinereus). Proc Natl Acad Sci U A. 2010/06/16.
621 2010;107(26):11889–94.

622 20. Lau AY-T, Cheng X, Cheng CK, Nong W, Cheung MK, Chan RH-F, et al. Discovery of
623 microRNA-like RNAs during early fruiting body development in the model mushroom
624 Coprinopsis cinerea. bioRxiv [Internet]. 2018 May 17 [cited 2019 Feb 3]; Available from:
625 http://biorxiv.org/lookup/doi/10.1101/325217

626 21. Martin F, Aerts A, Ahrén D, Brun A, Danchin EGJ, Duchaussoy F, et al. The genome of
627 Laccaria bicolor provides insights into mycorrhizal symbiosis. Nature. 2008
628 Mar;452(7183):88–92.

629 22. Nagy LG, Riley R, Tritt A, Adam C, Daum C, Floudas D, et al. Comparative genomics of
630 early-diverging mushroom-forming fungi provides insights into the origins of
631 lignocellulose decay capabilities. Mol Biol Evol. 2016;33(4):959–70.

632 23. Gehrmann T, Pelkmans JF, Lugones LG, Wösten HAB, Abeel T, Reinders MJT.
633 Schizophyllum commune has an extensive and functional alternative splicing repertoire. Sci
634 Rep. 2016;6.

635 24. Pelkmans JF, Patil MB, Gehrmann T, Reinders MJT, Wösten HAB, Lugones LG.
636 Transcription factors of schizophyllum commune involved in mushroom formation and
637 modulation of vegetative growth. Sci Rep. 2017;7(1).

638 25. Lugones LG, Scholtmeyer K. An abundant hydrophobin (ABHI) forms hydrophobic rodlet
639 layers in Agarics bisporus fruiting bodies. 2019;9.

640 26. Bayry J, Aimanianda V, Latge P. Hydrophobins—Unique Fungal Proteins. PLoS Pathog.
641 2012;8(5):4.

642 27. Wösten HAB, van Wetter M-A, Lugones LG, van der Mei HC, Busscher HJ, Wessels JGH.
643 How a fungus escapes the water to grow into the air. Curr Biol. 1999 Jan;9(2):85–8.

644 28. Liu Y, Boulianne RP, Lu BC, Kües U, Aebi M. Fruiting body development in Coprinus
645 cinereus: regulated expression of two galectins secreted by a non-classical pathway.
646 Microbiology. 2000 Aug 1;146(8):1841–53.

29. Hassan M, Rouf R, Tiralongo E, May T, Tiralongo J. Mushroom Lectins: Specificity, Structure and Bioactivity Relevant to Human Disease. Int J Mol Sci. 2015 Apr 8;16(12):7802–38.

30. Cooper DNW, Boulianne RP, Charlton S, Farrell EM, Sucher A, Lu BC. Fungal Galectins, Sequence and Specificity of Two Isolectins from *Coprinus cinereus*. J Biol Chem. 1997 Jan 17;272(3):1514–21.

31. Konno N, Sakamoto Y. An endo-β-1,6-glucanase involved in Lentinula edodes fruiting body autolysis. Appl Microbiol Biotechnol. 2011 Sep;91(5):1365–73.

32. Wessels GH. DEVELOPMENTAL REGULATION OF FUNGAL CELL WALL FORMATION. Annu Rev Phytopathol. 1994;32:413–37.

33. Fukuda K, Hiraga M, Asakuma S, Arai I, Sekikawa M, Urashima T. Purification and Characterization of a Novel Exo-β-1,3-1,6-glucanase from the Fruiting Body of the Edible Mushroom Enoki (*Flammulina velutipes*). Biosci Biotechnol Biochem. 2008 Dec 23;72(12):3107–13.

34. Liu Y. An Essential Gene for Fruiting Body Initiation in the Basidiomycete Coprinopsis cinerea Is Homologous to Bacterial Cyclopropane Fatty Acid Synthase Genes. Genetics. 2005 Nov 4;172(2):873–84.

35. Masuda R, Iguchi N, Tukuta K, Nagoshi T, Kemuriyama K, Muraguchi H. The Coprinopsis cinerea Tup1 homologue Cag1 is required for gill formation during fruiting body morphogenesis. Biol Open. 2016 Dec;5(12):1844–52.

667 36. Cheng CK, Au CH, Wilke SK, Stajich JE, Zolan ME, Pukkila PJ, et al. 5'-Serial Analysis
668 of Gene Expression studies reveal a transcriptomic switch during fruiting body
669 development in Coprinopsis cinerea. BMC Genomics. 2013;14(1):195.

670 37. de Sena-Tomas C, Navarro-Gonzalez M, Kues U, Perez-Martin J. A DNA Damage
671 Checkpoint Pathway Coordinates the Division of Dikaryotic Cells in the Ink Cap
672 Mushroom Coprinopsis cinerea. Genetics. 2013 Sep 1;195(1):47–57.

673 38. Kontkanen H, Westerholm-Parvinen A, Saloheimo M, Bailey M, Ratto M, Mattila I, et al.
674 Novel Coprinopsis cinerea Polyesterase That Hydrolyzes Cutin and Suberin. Appl Environ
675 Microbiol. 2009 Apr 1;75(7):2148–57.

676 39. Martins I, Hartmann DO, Alves PC, Martins C, Garcia H, Leclercq CC, et al. Elucidating
677 how the saprophytic fungus Aspergillus nidulans uses the plant polyester suberin as carbon
678 source. BMC Genomics. 2014;15(1):613.

679 40. Gonçalves HB, Riul AJ, Quiapim AC, Jorge JA, Guimarães LHS. Characterization of a
680 thermostable extracellular tannase produced under submerged fermentation by Aspergillus
681 ochraceus. Electron J Biotechnol [Internet]. 2012 Aug 8 [cited 2019 Feb 3];15(5). Available
682 from: http://www.ejbiotechnology.info/index.php/ejbiotechnology/article/view/946

683 41. Breschi A, Gingeras TR, Guigó R. Comparative transcriptomics in human and mouse. Nat
684 Rev Genet. 2017 May 8;18(7):425–40.

685 42. Song H-Y, Kim D-H, Kim J-M. Comparative transcriptome analysis of dikaryotic mycelia
686 and mature fruiting bodies in the edible mushroom Lentinula edodes. Sci Rep [Internet].
687 2018 Dec [cited 2019 Feb 3];8(1). Available from: http://www.nature.com/articles/s41598-
688 018-27318-z

689 43. Rahmad N, Al-Obaidi JR, Rashid NM, Zean N, Yusoff MHY, Shaharuddin N, et al.
690 Comparative proteomic analysis of different developmental stages of the edible mushroom
691 Termitomyces heimii. Biol Res. 2014;47(1):30.

692 44. Saboti J. Aspartic Proteases from Basidiomycete Clitocybe nebularis. Croat Chem Acta.
693 2009;7.

694 45. Banerjee G, Robertson DL, Leonard TJ. Hydrophobins Sc3 and Sc4 gene expression in
695 mounds, fruiting bodies and vegetative hyphae of Schizophyllum commune. Fungal Genet
696 Biol. 2008 Mar;45(3):171–9.

697 46. Wetter M-A, Schuren FHJ, Schuurs TA, Wessels JGH. Targeted mutation of the SC3
698 hydrophobin gene of Schizophyllum commune affects formation of aerial hyphae. FEMS
699 Microbiol Lett. 1996 Jul;140(2–3):265–9.

700 47. van Wetter M-A, Wösten HA., Sietsma JH, Wessels JG. Hydrophobin Gene Expression
701 Affects Hyphal Wall Composition in Schizophyllum commune. Fungal Genet Biol. 2000
702 Nov;31(2):99–104.

703 48. Baccelli I. Cerato-platanin family proteins: one function for multiple biological roles? Front
704 Plant Sci. 2014;5:769.

705 49. Tovar-Herrera OE, Batista-García RA, Sánchez-Carbente MDR, Iracheta-Cárdenas MM,
706 Arévalo-Niño K, Folch-Mallol JL. A novel expansin protein from the white-rot fungus
707 Schizophyllum commune. PLoS ONE. 2015;10(3).

50. Costachel C, Coddeville B, Latgé J-P, Fontaine T. Glycosylphosphatidylinositol-anchored Fungal Polysaccharide in *Aspergillus fumigatus*. J Biol Chem. 2005 Dec 2;280(48):39835–42.

51. Lussier M, Sdicu A-M, Shahinian S, Bussey H. The Candida albicans KRE9 gene is required for cell wall -1,6-glucan synthesis and is essential for growth on glucose. Proc Natl Acad Sci. 1998 Aug 18;95(17):9825–30.

52. Brown JL, Bussey H. The Yeast KRE9 Gene Encodes an 0 Glycoprotein Involved in Cell Surface ,-Glucan Assembly. MOL CELL BIOL. 1993;13:11.

53. Robledo-Briones M, Ruiz-Herrera J. Regulation of genes involved in cell wall synthesis and structure during Ustilago maydis dimorphism. FEMS Yeast Res. 2013;13(1):74–84.

54. Szeto CY, Leung GS, Kwan HS. Le.MAPK and its interacting partner, Le.DRMIP, in fruiting body development in Lentinula edodes. Gene. 2007/03/27. 2007;393(1–2):87–93.

55. Park Y-J, Baek JH, Lee S, Kim C, Rhee H, Kim H, et al. Whole Genome and Global Gene Expression Analyses of the Model Mushroom Flammulina velutipes Reveal a High Capacity for Lignocellulose Degradation. Schmoll M, editor. PLoS ONE. 2014 Apr;9(4):e93560.

56. Zhang J, Ren A, Chen H, Zhao M, Shi L, Chen M, et al. Transcriptome Analysis and Its Application in Identifying Genes Associated with Fruiting Body Development in Basidiomycete Hypsizygus marmoreus. Nowrousian M, editor. PLOS ONE. 2015 Apr;10(4):e0123025.

728 57. Wang M, Gu B, Huang J, Jiang S, Chen Y, Yin Y, et al. Transcriptome and Proteome
729 Exploration to Provide a Resource for the Study of Agrocybe aegerita. Carter DA, editor.
730 PLoS ONE. 2013 Feb 13;8(2):e56686.

731 58. Sakamoto Y, Nakade K, Sato S, Yoshida K, Miyazaki K, Natsume S, et al. Lentinula
732 edodes Genome Survey and Postharvest Transcriptome Analysis. Appl Environ Microbiol.
733 2017 15;83(10).

734 59. Sakamoto Y, Irie T, Sato T. Isolation and characterization of a fruiting body-specific exo-
735 beta-1,3-glucanase-encoding gene, exg1, from Lentinula edodes. Curr Genet. 2005
736 Apr;47(4):244–52.

737 60. Ene IV, Walker LA, Schiavone M, Lee KK, Martin-Yken H, Dague E, et al. Cell Wall
738 Remodeling Enzymes Modulate Fungal Cell Wall Elasticity and Osmotic Stress Resistance.
739 mBio [Internet]. 2015 Sep 1 [cited 2019 Feb 3];6(4). Available from:
740 http://mbio.asm.org/lookup/doi/10.1128/mBio.00986-15

741 61. Hurtado-Guerrero R, Schüttelkopf AW, Mouyna I, Ibrahim AFM, Shepherd S, Fontaine T,
742 et al. Molecular Mechanisms of Yeast Cell Wall Glucan Remodeling. J Biol Chem. 2009
743 Mar 27;284(13):8461–9.

744 62. Sakamoto Y, Watanabe H, Nagai M, Nakade K, Takahashi M, Sato T. Lentinula edodes
745 tlg1 encodes a thaumatin-like protein that is involved in lentinan degradation and fruiting
746 body senescence. Plant Physiol. 2006;141:793–801.

747 63. Busch S, Braus GH. How to build a fungal fruit body: from uniform cells to specialized
748 tissue. Mol Microbiol. 2007;64(4):873–6.

749 64. Buser R, Lazar Z, Käser S, Künzler M, Aebi M. Identification, Characterization, and
750 Biosynthesis of a Novel *N* -Glycan Modification in the Fruiting Body of the Basidiomycete
751 *Coprinopsis cinerea*. J Biol Chem. 2010 Apr 2;285(14):10715–23.

752 65. Plaza D, Lin C-W, van der Velden NS, Aebi M, Künzler M. Comparative transcriptomics
753 of the model mushroom Coprinopsis cinerea reveals tissue-specific armories and a
754 conserved circuitry for sexual development. BMC Genomics. 2014;15(1):492.

755 66. Rajam MV, Chandola N, Saiprasad Goud P, Singh D, Kashyap V, Choudhary ML, et al.
756 Thaumatin gene confers resistance to fungal pathogens as well as tolerance to abiotic
757 stresses in transgenic tobacco plants. Biol Plant. 2007 Mar;51(1):135–41.

758 67. Zhang Y, Yan H, Wei X, Zhang J, Wang H, Liu D. Expression analysis and functional
759 characterization of a pathogen-induced thaumatin-like gene in wheat conferring enhanced
760 resistance to *Puccinia triticina*. J Plant Interact. 2017 Jan;12(1):332–9.

761 68. Zhang J, Wang F, Liang F, Zhang Y, Ma L, Wang H, et al. Functional analysis of a
762 pathogenesis-related thaumatin-like protein gene TaLr35PR5 from wheat induced by leaf
763 rust fungus. BMC Plant Biol [Internet]. 2018 Dec [cited 2019 Feb 3];18(1). Available from:
764 https://bmcplantbiol.biomedcentral.com/articles/10.1186/s12870-018-1297-2

765 69. Grenier J, Potvin C, Asselin A. Some Fungi Express beta-1,3-Glucanases Similar to
766 Thaumatin-like Proteins. Mycologia. 2000 Sep;92(5):841.

767 70. Chen H, Kovalchuk A, Keriö S, Asiegbu FO. Distribution and bioinformatic analysis of the
768 cerato-platanin protein family in Dikarya. Mycologia. 2013 Nov;105(6):1479–88.

769 71. Gaderer R, Bonazza K, Seidl-Seiboth V. Cerato-platanins: A fungal protein family with
770 intriguing properties and application potential. Vol. 98, Applied Microbiology and
771 Biotechnology. 2014. p. 4795–803.

772 72. Boraston AB, Tomme P, Amandoron EA, Kilburn DG. A novel mechanism of xylan
773 binding by a lectin-like module from Streptomyces lividans xylanase 10A. 2000;9.

774 73. Fujimoto Z. Structure and Function of Carbohydrate-Binding Module Families 13 and 42 of
775 Glycoside Hydrolases, Comprising a β-Trefoil Fold. Biosci Biotechnol Biochem. 2013 Jul
776 23;77(7):1363–71.

777 74. Schubert M, Bleuler-Martinez S, Butschi A, Wälti MA, Egloff P, Stutz K, et al. Plasticity of
778 the β-trefoil protein fold in the recognition and control of invertebrate predators and
779 parasites by a fungal defence system. PLoS Pathog. 2012;8(5).

780 75. Collins T, Stone JR, Williams AJ. All in the Family: the BTB/POZ, KRAB, and SCAN
781 Domains. Mol Cell Biol. 2001 Jun 1;21(11):3609–15.

782 76. Connelly C, Hieter P. Budding Yeast SKP1 Encodes an Evolutionarily Conserved
783 Kinetochore Protein Required for Cell Cycle Progression. Cell. 1996 Jul;86(2):275–85.

784 77. Pelkmans JF, Vos AM, Scholtmeijer K, Hendrix E, Baars JJP, Gehrmann T, et al. The
785 transcriptional regulator c2h2 accelerates mushroom formation in Agaricus bisporus. Appl
786 Microbiol Biotechnol. 2016;100(16):7151–9.

787 78. Morin E, Kohler A, Baker AR, Foulongne-Oriol M, Lombard V, Nagy LG, et al. Genome
788 sequence of the button mushroom Agaricus bisporus reveals mechanisms governing

adaptation to a humic-rich ecological niche. Proc Natl Acad Sci U S A. 2012 Oct 23;109(43):17501–6.

79. Zhou Y, Chen L, Fan X, Bian Y. De Novo Assembly of Auricularia polytricha Transcriptome Using Illumina Sequencing for Gene Discovery and SSR Marker Identification. Freitag M, editor. PLoS ONE. 2014 Mar 13;9(3):e91740.

80. Endo H, Kajiwara S, Tsunoka O, Shishido K. A novel cDNA, priBc, encoding a protein with a Zn(II)2Cys6 zinc cluster DNA-binding motif, derived from the basidiomycete Lentinus edodes. Gene. 1994 Feb 11;139(1):117–21.

81. Miyazaki Y, Tsunoka O, Shishido K. Determination of the DNA-Binding Sequences of the Zn(II)2Cys6 Zinc-Cluster-Containing PRIB Protein, Derived from the Basidiomycete Lentinus edodes Gene. J Biochem (Tokyo). 1997 Dec 1;122(6):1088–91.

82. Muraguchi H, Fujita T, Kishibe Y, Konno K, Ueda N, Nakahori K, et al. The exp1 gene essential for pileus expansion and autolysis of the inky cap mushroom Coprinopsis cinerea (Coprinus cinereus) encodes an HMG protein. Fungal Genet Biol. 2008 Jun;45(6):890–6.

83. Trail F, Wang Z, Stefanko K, Cubba C, Townsend JP. The ancestral levels of transcription and the evolution of sexual phenotypes in filamentous fungi. Fraser HB, editor. PLOS Genet. 2017 Jul 13;13(7):e1006867.

84. Pellegrin C, Morin E, Martin FM, Veneault-Fourrey C. Comparative Analysis of Secretomes from Ectomycorrhizal Fungi with an Emphasis on Small-Secreted Proteins. Front Microbiol. 2015 Nov;6:1278.

809 85. de Freitas Pereira M, Veneault-Fourrey C, Vion P, Guinet F, Morin E, Barry KW, et al.
810 Secretome Analysis from the Ectomycorrhizal Ascomycete Cenococcum geophilum. Front
811 Microbiol [Internet]. 2018 Feb 13 [cited 2019 Feb 3];9. Available from:
812 http://journal.frontiersin.org/article/10.3389/fmicb.2018.00141/full

813 86. Pellegrin C, Daguerre Y, Ruytinx J, Guinet F, Kemppainen M, Plourde MB, et al. Laccaria
814 bicolor MiSSP8 is a small-secreted protein decisive for the establishment of the
815 ectomycorrhizal symbiosis. bioRxiv [Internet]. 2017 Dec 4 [cited 2019 Feb 3]; Available
816 from: http://biorxiv.org/lookup/doi/10.1101/218131

817 87. Feldman D, Kowbel DJ, Glass NL, Yarden O, Hadar Y. A role for small secreted proteins
818 (SSPs) in a saprophytic fungal lifestyle: Ligninolytic enzyme regulation in Pleurotus
819 ostreatus. Sci Rep. 2017;7(1).

820 88. Grabherr MG, Haas BJ, Yassour M, Levin JZ, Thompson DA, Amit I, et al. Full-length
821 transcriptome assembly from RNA-Seq data without a reference genome. Nat Biotechnol.
822 2011 May 15;29(7):644–52.

823 89. Grigoriev I V, Nikitin R, Haridas S, Kuo A, Ohm R, Otillar R, et al. MycoCosm portal:
824 Gearing up for 1000 fungal genomes. Nucleic Acids Res. 2014;42(D1).

825 90. Robinson MD, McCarthy DJ, Smyth GK. edgeR: a Bioconductor package for differential
826 expression analysis of digital gene expression data. Bioinforma Oxf Engl. 2010;26(1):139–
827 40.

828 91. Ritchie ME, Phipson B, Wu D, Hu Y, Law CW, Shi W, et al. Limma powers differential
829 expression analyses for RNA-sequencing and microarray studies. Nucleic Acids Res.
830 2015;43(7):e47.

831 92. Katoh K, Standley DM. MAFFT multiple sequence alignment software version 7:
832 improvements in performance and usability. Mol Biol Evol. 2013 Apr;30(4):772–80.

833 93. Emms DM, Kelly S. OrthoFinder: solving fundamental biases in whole genome
834 comparisons dramatically improves orthogroup inference accuracy. Genome Biol [Internet].
835 2015 Dec [cited 2019 Feb 4];16(1). Available from:
836 http://genomebiology.com/2015/16/1/157

837 94. Lombard V, Golaconda Ramulu H, Drula E, Coutinho PM, Henrissat B. The carbohydrate-
838 active enzymes database (CAZy) in 2013. Nucleic Acids Res. 2014;42(D1).

839 95. Revell LJ. SIZE-CORRECTION AND PRINCIPAL COMPONENTS FOR
840 INTERSPECIFIC COMPARATIVE STUDIES. Evolution. 2009 Dec;63(12):3258–68.

841 96. Revell LJ. phytools: An R package for phylogenetic comparative biology (and other
842 things). Methods Ecol Evol. 2012;3(2):217–23.

843 97. Hanks SK, Hunter T. Protein kinases 6. The eukaryotic protein kinase superfamily: kinase
844 (catalytic) domain structure and classification. FASEB J Off Publ Fed Am Soc Exp Biol.
845 1995 May;9(8):576–96.

846 98. Manning G, Whyte DB, Martinez R, Hunter T, Sudarsanam S. The protein kinase
847 complement of the human genome. Vol. 298, Science. 2002. p. 1912–34.

848 99. Petersen TN, Brunak S, Von Heijne G, Nielsen H. SignalP 4.0: Discriminating signal
849 peptides from transmembrane regions. Vol. 8, Nature Methods. 2011. p. 785–6.

850 100. Horton P, Park KJ, Obayashi T, Fujita N, Harada H, Adams-Collier CJ, et al. WoLF
851 PSORT: Protein localization predictor. Nucleic Acids Res. 2007;35(SUPPL.2).

852 101. Krogh A, Larsson B, von Heijne G, Sonnhammer EL. Predicting transmembrane protein
853 topology with a hidden Markov model: application to complete genomes. J Mol Biol. 2001
854 Jan 19;305(3):567–80.

855

856 # Figure Legends

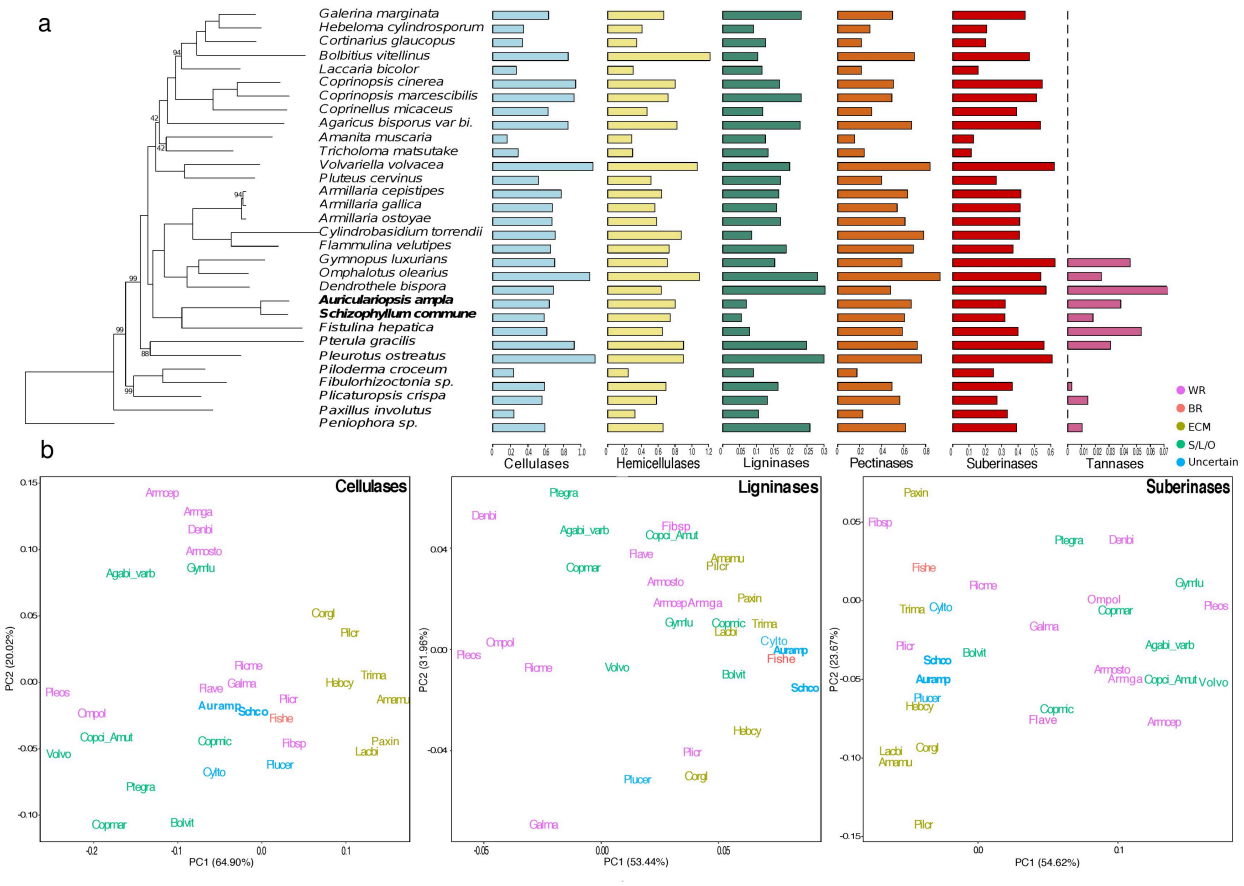

857

858 **Figure 1.** Phylogenetic relationships and lignocellulose degrading gene repertoire of *A. ampla*
859 compared to *S. commune* and 29 other Agaricomycetes. A, species tree showing the phylogenetic
860 affinities of the Schizophyllaceae (bold, left panel) and copy number distribution of cellulose,
861 hemicellulose, pectin, lignin degrading gene families as well as those of putative suberinases and
862 tannases. B, phylogenetic principal component analyses of cellulose, lignin and suberin
863 degrading enzymes. Species names colored based on nutritional mode (WR - white rot, BR -

brown rot, ECM - ectomycorrhizal, S/L/O - soil and litter decomposer, Uncertain - nutritional mode not known with certainty). For better visibility, a few species have been moved slightly on the plots (information in Supplementary Table 5) See also Supplementary Figure 1 for original plots.

Figure 2. Fruiting bodies and developmental stages of *A. ampla* and *S. commune*. Developmental stages are indicated on each panel. A, fruiting bodies of *A. ampla* produced in vitro, on sections of barked poplar logs plugged into malt-extract agar. B and C, fruiting bodies of *A. ampla* and *S. commune* in their natural habitat. D, cross sections of developmental stages of *A. ampla*: left - stage 1 primordium (left), stage 2 primordium (middle) and mature fruiting body (right). E, Cross section of a mature fruiting body of *S. commune*, showing congregated single fruiting bodies.

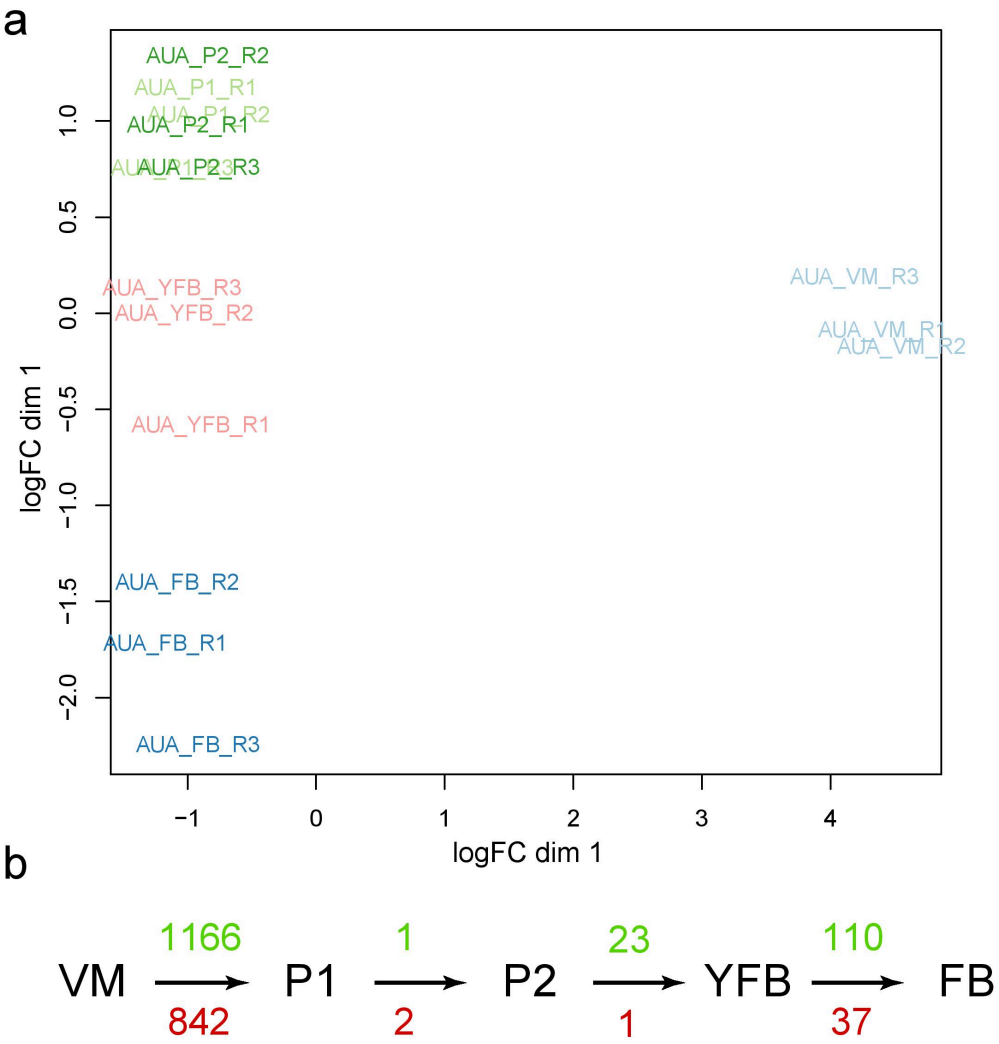

Figure 3. Overview of the developmental transcriptome of *A. ampla*. A, Multi-dimensional scaling for RNA-Seq replicates from 5 developmental stages of *Auriculariopsis ampla*. Biological replicates belonging to similar tissue type group together. The replicates for P1 and P2 cluster together and remaining developmental stages keep apart. B, Graphical representation of number of significantly upregulated (green) and downregulated (red) genes among developmental stages and tissue types in *A. ampla*.

Abbreviations: VM - vegetative mycelium, P1 - stage 1 primordium, P2 - stage 2 primordium, YFB - young fruiting body, FB - mature fruiting body.

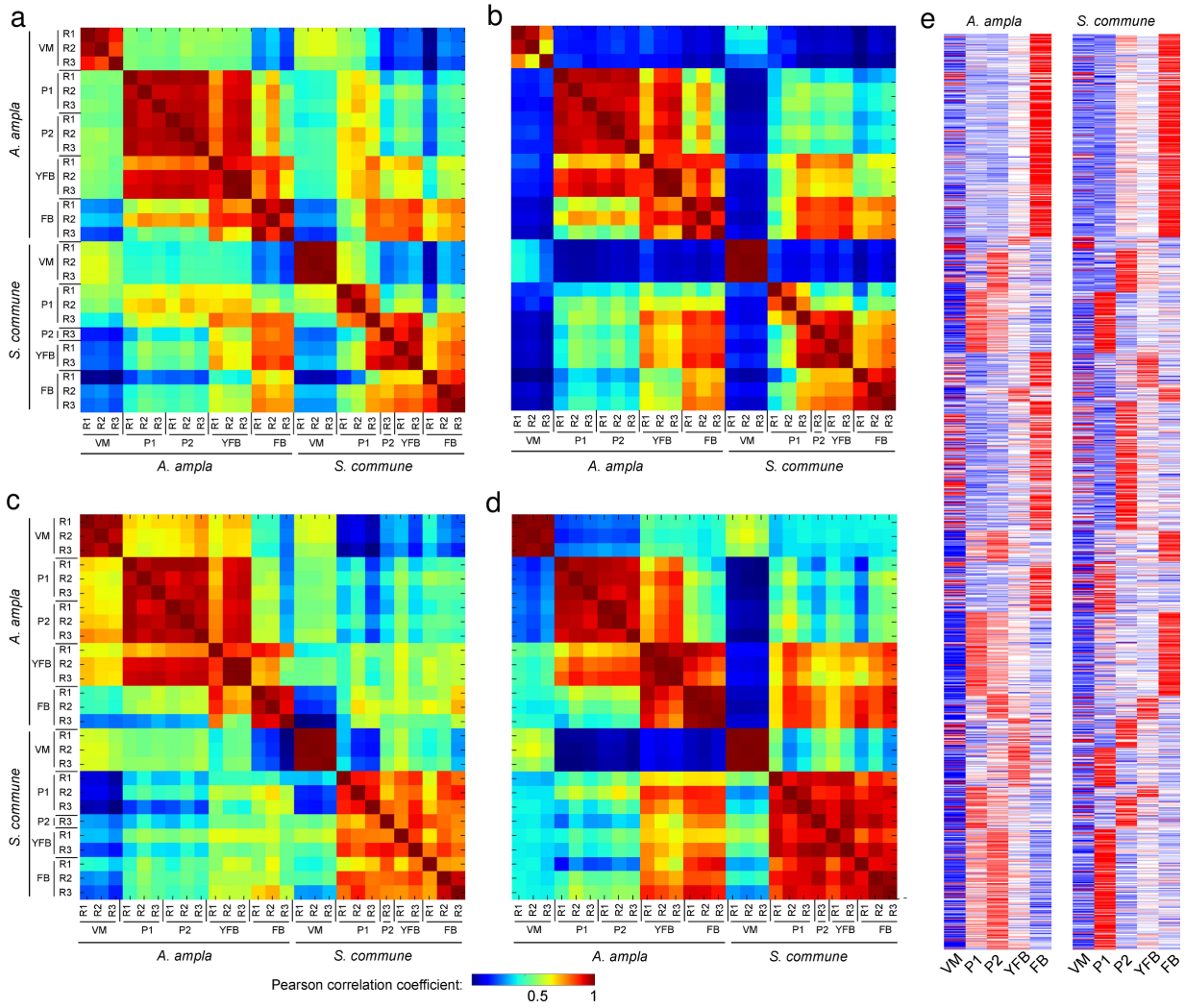

Figure 4. Global transcriptome similarity between developmental transcriptomes of *A. ampla* and *S. commune*. Pearson correlation coefficient-based heatmaps show similarity among developmental stages of the two species for all 7369 co-orthologs (A), for 1182 developmentally regulated co-orthologs (B), for 252 co-orthologous transcription factor pairs (C) and 42 developmentally regulated co-orthologous TF pairs (D). Warmer color indicates higher similarity. Biological replicates are indicated next to the heatmap (R1-R3). E, paired heatmap of gene expression (FPKM) for 7369 co-orthologous gene pairs between *A. ampla* and *S. commune*. Developmental stages for both species are as follows: VM - vegetative mycelium, P1 - stage 1 primordium, P2 - stage 2 primordium, YFB - young fruiting body, FB - mature fruiting body.

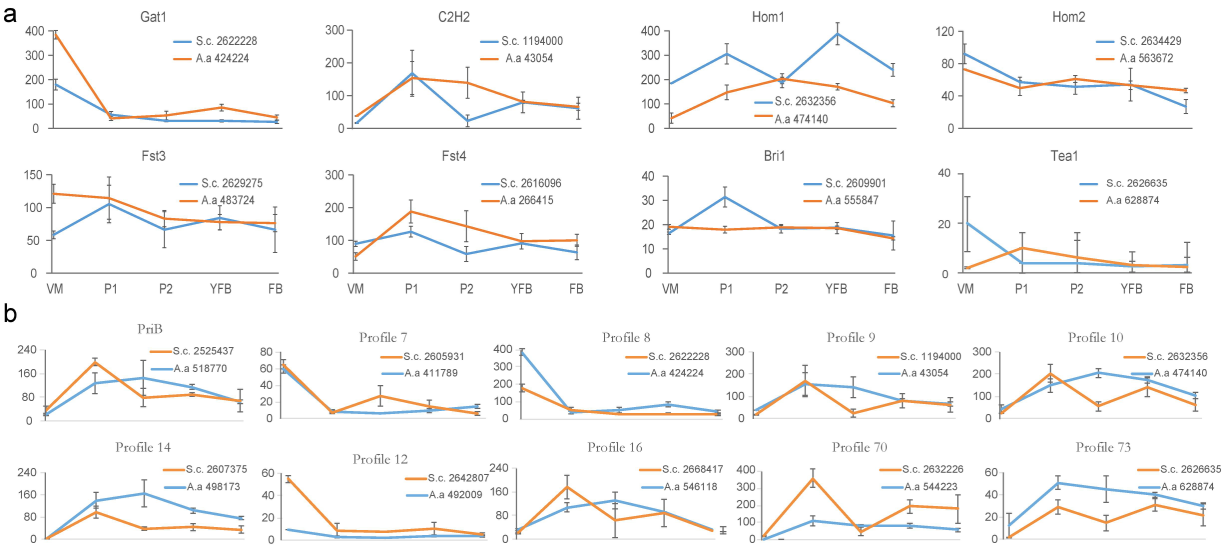

Figure 5. The expression patterns of developmentally regulated co-orthologous transcription factors and their similarity across the two species. A, Expression patterns for 8 previously characterized TFs in *S. commune* and *A. ampla*. B, developmentally regulated co-orthologous TFs in the two species with high expression dynamics during fruiting body development. *S. commune* and *A. ampla* genes are shown by blue and orange lines respectively.

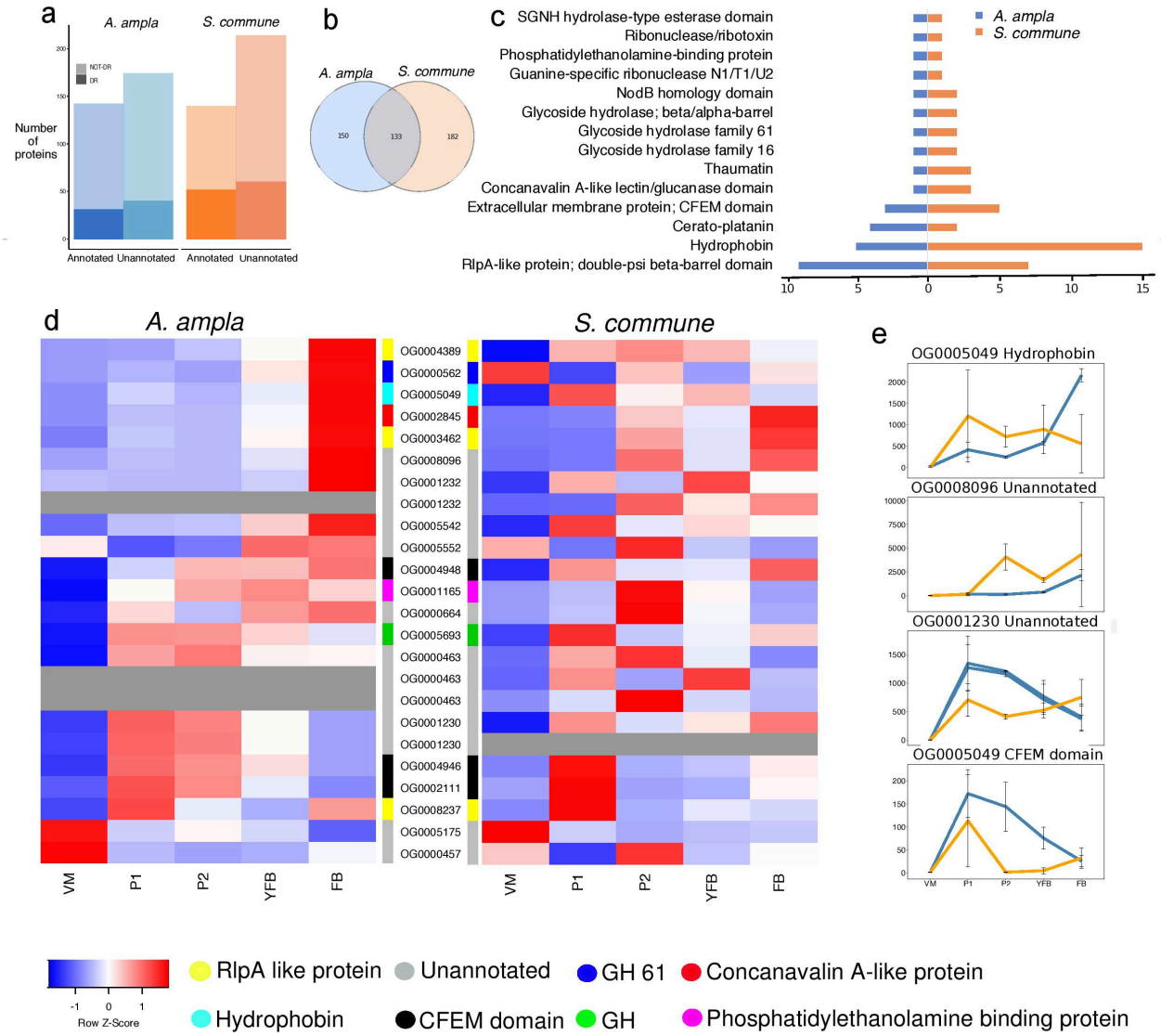

Figure 6. Small secreted proteins in fruiting body transcriptomes. A, The repertoires of annotated vs unannotated and developmentally regulated (DR) vs. non-developmentally regulated (NOT-DR) SSPs in fruiting body transcriptomes of *A. ampla* and *S. commune*. B, Venn-diagram depicting orthology relationships among SSPs of the two species. Number in each cell represent the number of shared or species-specific orthogroups. C, functional annotation terms (InterPro domains) present in SSPs of both *A. ampla* and *S. commune*. Terms specific to either species are not shown. D, expression heatmaps of co-orthologous SSPs in the two species.

909 Orthogroup IDs are shown next to rows. Blue and red correspond to low and high expression,
910 respectively. Greyed-out rows denote missing genes in orthogroup in which the 2 species did not
911 have the same number of genes. Color coded bar next to heatmap shows functional annotations
912 of the orthogroups. See Supplementary Figure 4 for heatmaps of species-specific genes. E,
913 expression profiles of genes in four of the orthogroups through development, including two
914 orthogroups of unannotated genes. Blue and orange denote *Auriculariopsis* and *Schizophyllum*
915 genes, respectively. Variances across the three biological replicates are shown at corresponding
916 developmental stages. See Supplementary Table 6 for protein IDs.

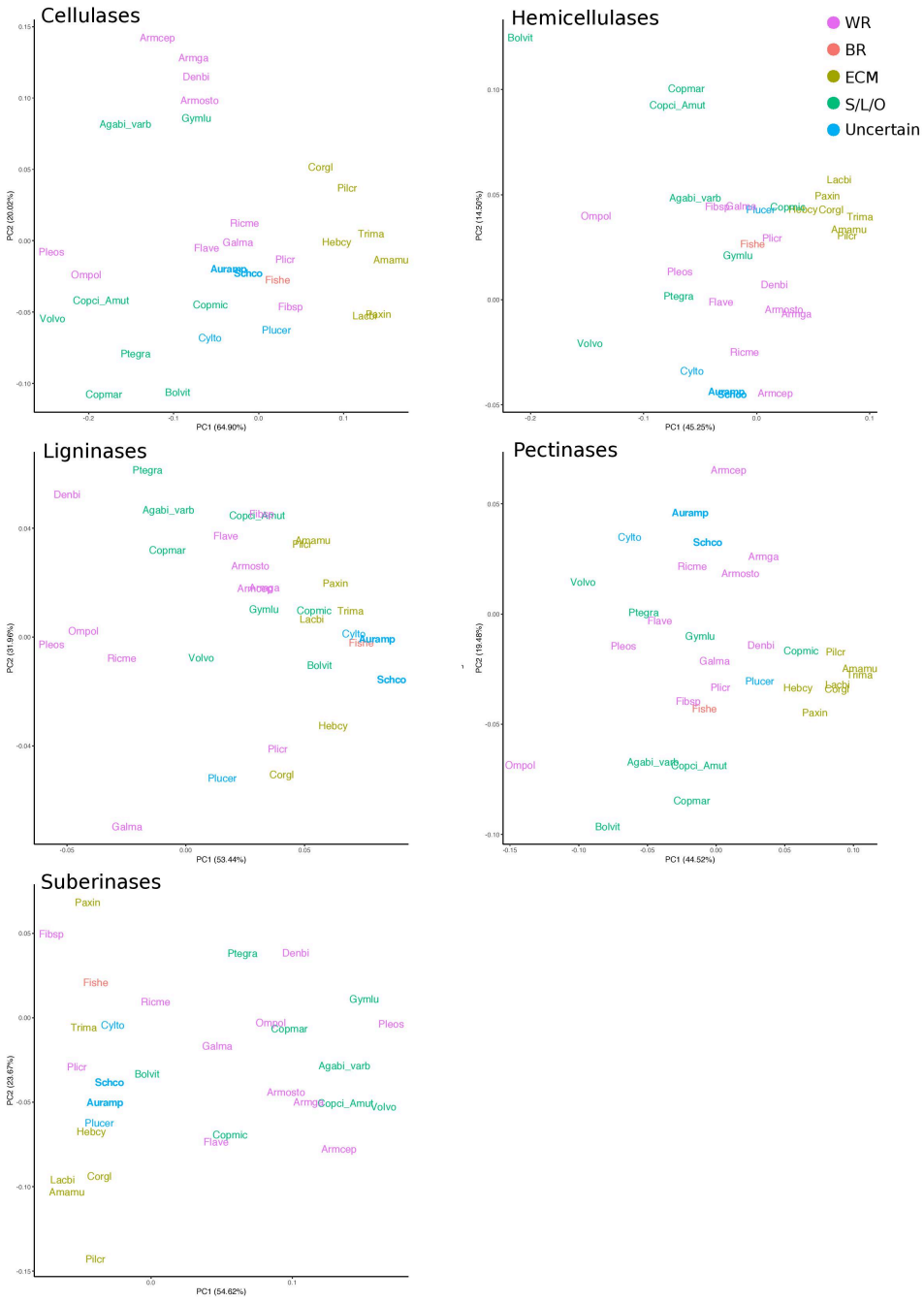

Supplementary Figure 1. Phylogenetic Principal Component Analysis (PCA) based on CAZyme family copy numbers in 31 species. CAZymes categorized into 5 substrates - cellulases, hemicellulases, ligninases, pectinases and putative suberinases and the copy numbers normalized according to their proteome sizes along with ML species tree were used for the phylogenetic PCA. Species have been colored according to their nutritional modes.

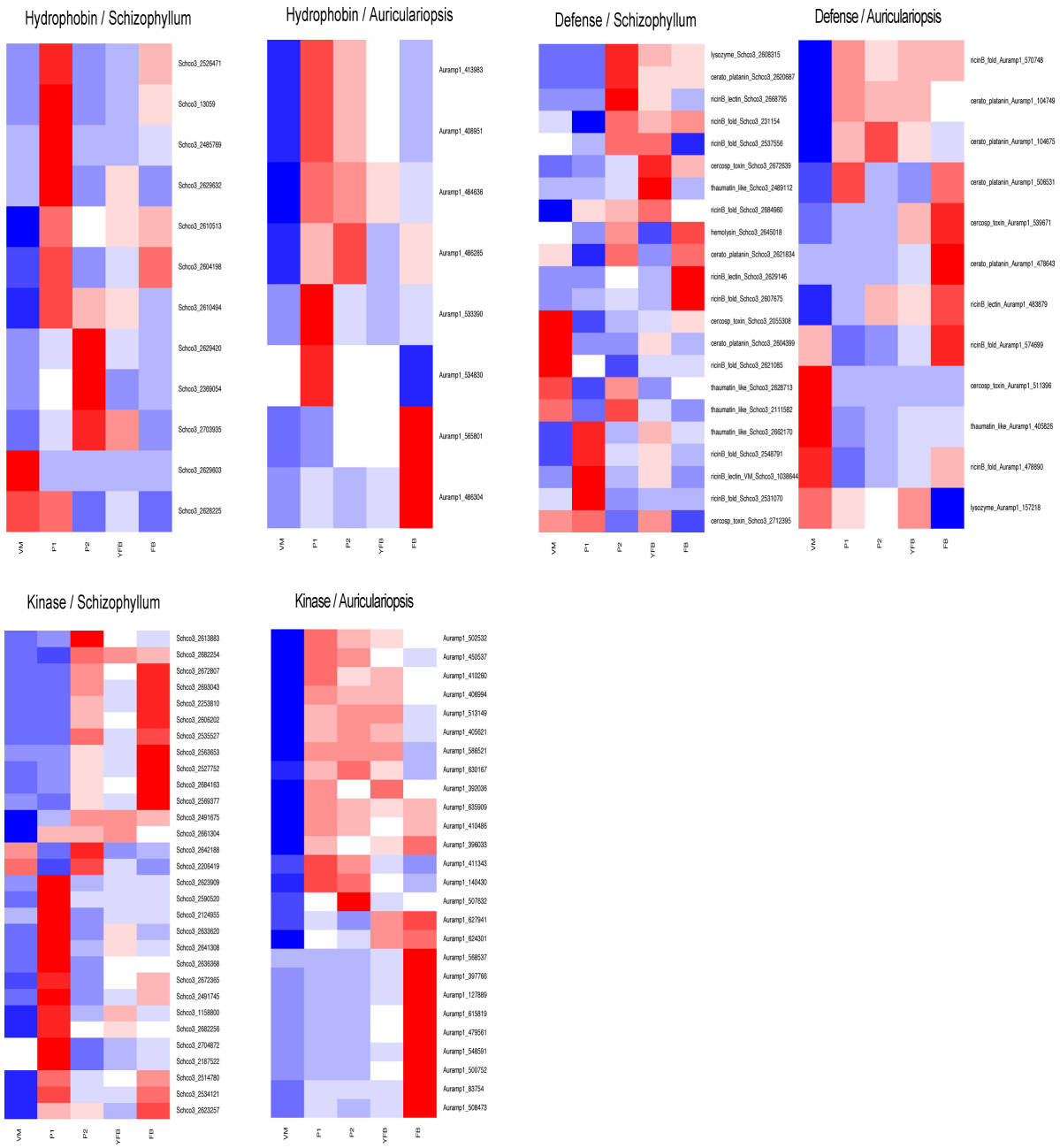

923

924 **Supplementary Figure 2.** Heatmaps of developmentally regulated genes for families having a
925 putative role in fruiting body formation. Developmental stages in both species are abbreviated
926 as 'VM' vegetative mycelium; 'P1' stage 1 primordium; 'P2' stage 2 primordium; 'YFB' young
927 fruiting body; and 'FB' fruiting body.

928

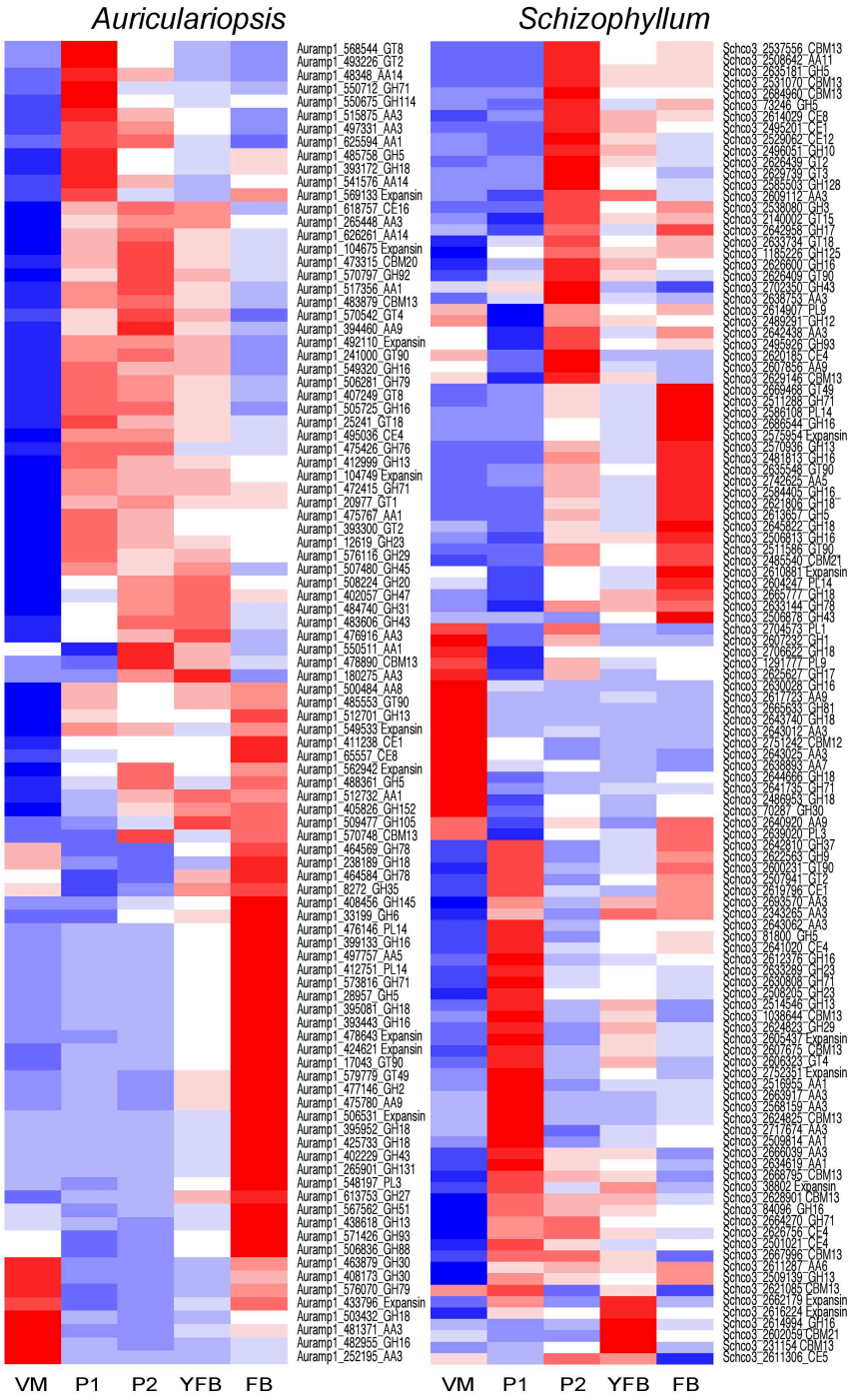

929

930 **Supplementary Figure 3.** Heatmaps of developmentally regulated Carbohydrate

931 Active Enzymes (CAZymes) in the two species. Abbreviations: 'VM' vegetative mycelium; 'P1'

932 stage 1 primordium; 'P2' stage 2 primordium; 'YFB' young fruiting body; and 'FB' fruiting

933 body.

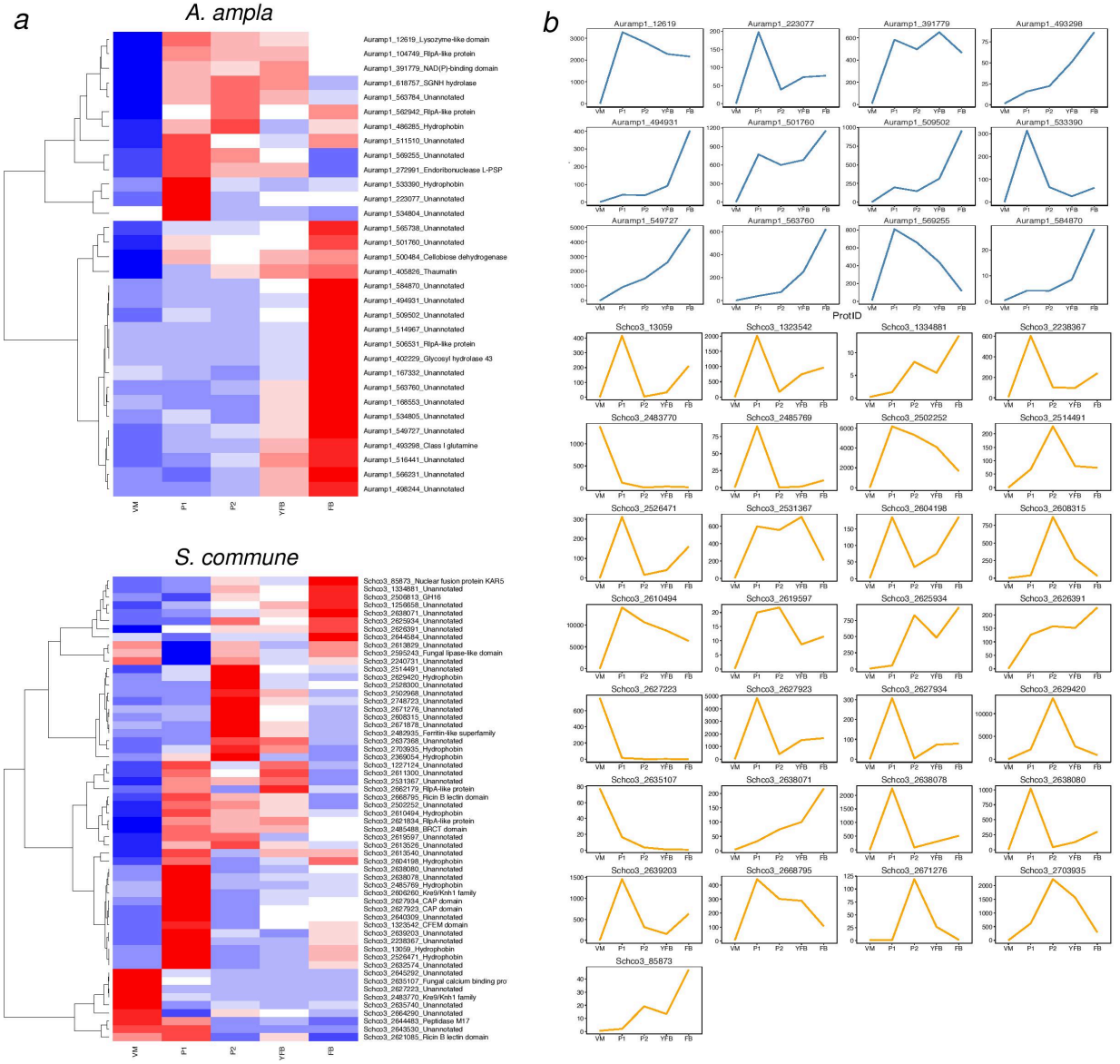

934

935 **Supplementary Figure 4.** Developmentally regulated and species-specific small secreted

936 proteins (SSPs) in the two species. A, Heatmaps of species specific SSPs in *A. ampla* (top) and *S.*

937 *commune* (bottom); B, expression profiles of genes having high expression dynamics (FC>50).

938 Genes in *A. ampla* and *S. commune* are shown in blue and orange respectively.